Remote Sensing of Environment 306 (2024) 114144

Contents lists available at ScienceDirect

Remote Sensing of Environment

journal homepage: www.elsevier.com/locate/rse

Multi-sensor satellite imagery reveals spatiotemporal changes in peatland water table after restoration

Aleksi Isoaho [a,b,*], Lauri Ikkala [b,c], Lassi Päkkilä [b], Hannu Marttila [b], Santtu Kareksela [d], Aleksi Räsänen [a,e]

[a] Natural Resources Institute Finland (Luke), Paavo Havaksen tie 3, FI-90570 Oulu, Finland
[b] Water, Energy and Environmental Engineering Research Unit, Faculty of Technology, University of Oulu, P.O. Box 4300, Oulu, Finland
[c] Geological Survey of Finland (GTK), Teknologiakatu 7, FI-67101 Kokkola, Finland
[d] Metsähallitus, Parks & Wildlife Finland, Vankanlahde 7, FI-13100 Hämeenlinna, Finland
[e] Geography Research Unit, Faculty of Science, University of Oulu, P.O. Box 8000, Oulu, Finland

ARTICLE INFO

Editor: Menghua Wang

Keywords:
Remote sensing
Optical
SAR
Monitoring
Machine learning
Hydrology

ABSTRACT

Remote sensing (RS) has been suggested as a tool to spatially monitor the status of peatland ecosystem functioning after restoration. However, there have been only a few studies in which post-restoration hydrological changes have been quantified with RS-based modelling. To address this gap, we developed an approach to assess post-restoration spatiotemporal changes in the peatland water table (WT) with optical (Sentinel-2 and Landsat 7–9) and radar (Sentinel-1) imagery. We tested the approach in eleven northern boreal peatlands (six restored, and five control sites) impacted by forestry drainage in northern Finland using Google Earth Engine cloud computing capabilities. We constructed a random forest regression model with spatiotemporal field-measured WT data as a dependent variable and satellite imagery features as independent variables. To assess the spatiotemporal changes, we constructed representative maps for situations before and after restoration, separately for early summer high-water and midsummer low-water conditions. To further quantify temporal changes during 2015–2023 and to test their statistical significance, we conducted a bootstrap hypothesis test for the areas near the restoration measures and similar areas in the control sites. The regression model had a relatively good fit and explanatory capacity (overall $R^2 = 0.71$, RMSE = 6.01 cm), while there were notable site-specific variations. The WT maps showed that the post-restoration changes were not uniform and concentrated near the restoration measures. The bootstrap test showed that the WT increased more in the restored areas (4.7–8.8 cm) than in the control areas (0.1–5.2 cm). Our results indicate that restoration impact on surface hydrology can be quantified with multi-sensor satellite imagery and a machine learning approach in treeless peatlands.

1. Introduction

Peatlands cover 3% of global land cover (Xu et al., 2018) and 11% of them are degraded, mainly due to drainage for forestry, agriculture and peat extraction (Leifeld and Menichetti, 2018). In pristine conditions, peatlands offer many critical ecosystem services and support biodiversity (Bonn et al., 2016), whereas degraded ones are known to negatively impact emissions (e.g. Leifeld and Menichetti, 2018; Wilkinson et al., 2023), leaching (e.g. Nieminen et al., 2017; Marttila et al., 2018) and local biodiversity (Chapman et al., 2003). Global peatland degradation has increased the pressure on restoration activities for gaining more pristine-like ecosystem structure and functions (e.g. Kareksela et al., 2015) and thus reversing drainage-induced negative effects. For instance, in the European Union, the proposed nature restoration law is likely to launch a significant increase in restoration actions on peatlands, especially in northern Europe (European Commission, 2023).

In typical boreal forestry-drained peatlands, artificial drainage networks decrease water table (WT) level in peat layers and increase WT fluctuation (Prevost et al., 1997; Haapalehto et al., 2014). Additionally, drainage disconnects the surface and near-surface water flow pathways with the surrounding catchment (Tahvanainen, 2011; Sallinen et al., 2019; Ikkala et al., 2022). This leads to peatland degradation as the water supply to the peat layers is limited (Holden et al., 2006). A lowered WT exposes peat to aerobic decomposition (Whittington and Price,

* Corresponding author at: Natural Resources Institute Finland (Luke), Paavo Havaksen tie 3, FI-90570 Oulu, Finland.
E-mail address: aleksi.isoaho@luke.fi (A. Isoaho).

https://doi.org/10.1016/j.rse.2024.114144
Received 30 October 2023; Received in revised form 26 March 2024; Accepted 27 March 2024
Available online 30 March 2024

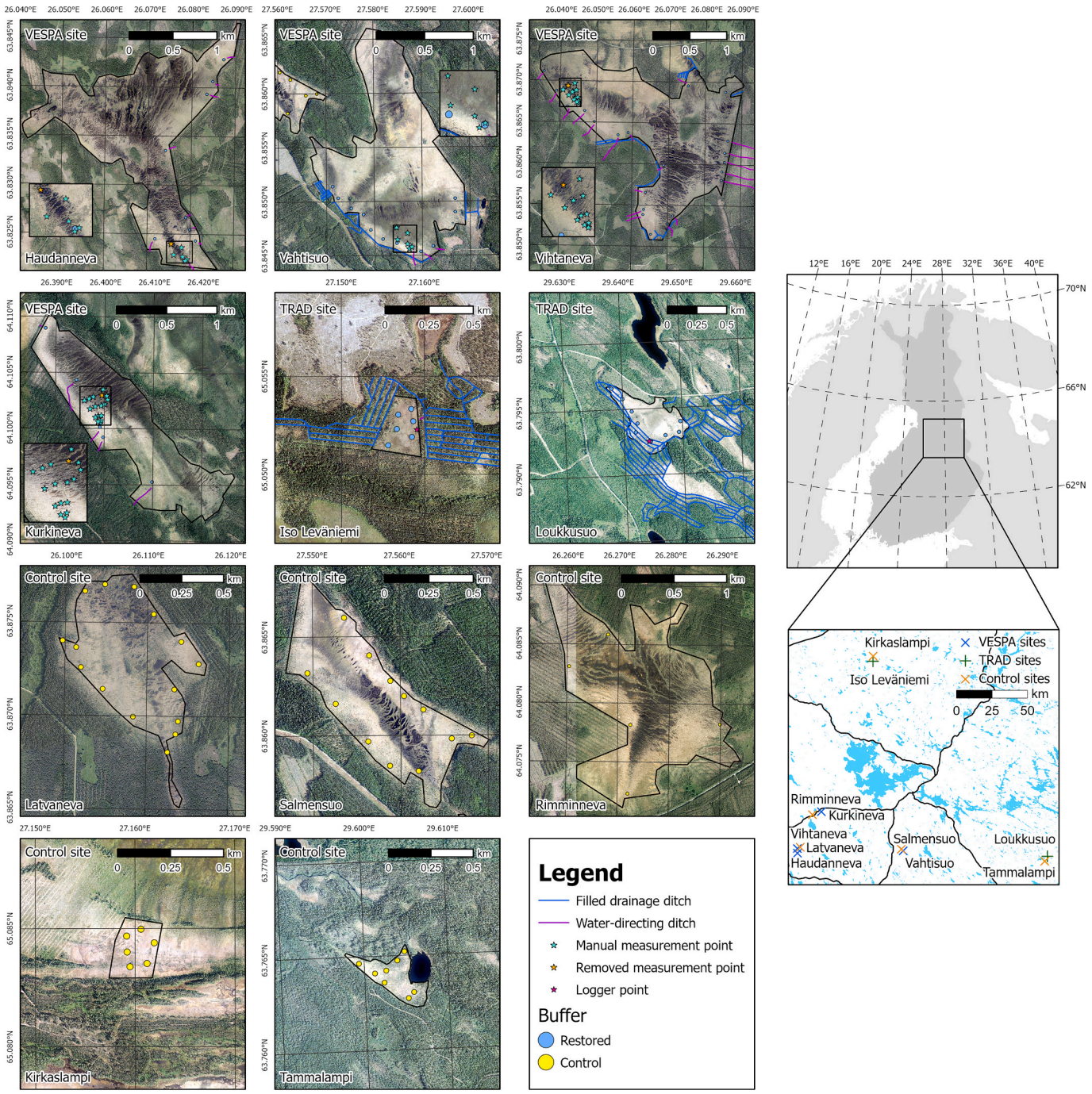

Fig. 1. The locations of the study sites, restoration measures, water table measurement points and buffers. Stars indicate manual and automatic logger water table measurement locations. Removed measurement points refer to points which were removed from the dataset used in the analyses (see section 2.2). Buffers for satellite data collection for statistical analyses (see section 2.5.2) are in true size. The scale between the sites varies; the grid size is identical for all sites. Location map contains main roads and water bodies for visibility. Aerial photos and topographic database are open data from National Land Survey of Finland, acquired between 2019 and 2024.

2006; Itoh et al., 2017), causing carbon dioxide emissions (Leifeld and Menichetti, 2018; Wilkinson et al., 2023) and increased leaching of nitrogen, phosphorus, and dissolved organic carbon to the downstream waterbodies (Nieminen et al., 2017; Marttila et al., 2018).

Traditionally, restoration of forestry-drained peatlands has particularly been conducted by damming and infilling ditches as well as harvesting trees to decrease local evaporation (Andersen et al., 2017). However, lately in Finland, restoration has also been conducted by directing the water flow routes to the unditched peatland areas (Autio et al., 2018; Kareksela et al., 2021; Isoaho et al., 2023) suffering from adjacent drainage (Sallinen et al., 2019). The restoration method has only recently been systematically introduced and lacks scientific knowledge regarding its efficiency (Isoaho et al., 2023).

Previously, the restoration impact and success have been assessed with point-based field measurements and monitoring such as standpipe wells and vegetation plots. In Finland, an increased WT has been the most commonly used indicator for hydrological changes which are usually the primary abiotic target in restoration actions (Haapalehto et al., 2014; Menberu et al., 2016). However, point-based monitoring measures do not account for the spatial variability in the restoration

Table 1
Study sites' climatic information, remote sensing monitoring area, restoration implementation times, implemented measures, field monitoring methods, and used control sites.

Study site	Haudanneva	Vahtisuo	Vihtaneva	Kurkineva	Iso Leväniemi	Loukkusuo
Annual mean temperature*	3.0 °C	2.8 °C	3.0 °C	2.9 °C	2.1 °C	2.3 °C
Annual precipitation*	638 mm	702 mm	638 mm	612 mm	625 mm	765 mm
Monitoring area	245 ha	189 ha	310 ha	133 ha	7 ha	19 ha
Restoration	Winter 2017–2018	Autumns 2018 and 2019	Autumn 2021	Winter 2021–2022	Autumn 2019	Summer 2020
Water-directing ditches	x	x	x	x	x	
Ditch infilling		x	x		x	x
Damming	x	x	x	x	x	x
Water table field monitoring method	Manual measurements	Manual measurements	Manual measurements	Manual measurements	Automatic loggers	Automatic loggers
Control site	Latvaneva	Salmensuo	Latvaneva	Rimminneva	Kirkaslampi	Tammalampi

* 1990–2020 average according to gridded climatology of Finland (Aalto et al., 2016; Finnish Meteorological Institute, 2023).

success and thus do not provide quantitative information on the impacted area (Haapalehto et al., 2014; Isoaho et al., 2023). Additionally, extensive field monitoring is usually resource-demanding and sometimes impossible as some peatlands can be practically inaccessible. Therefore, several studies have suggested remote sensing (RS) based monitoring as a method for investigating the quantitative effects of the peatland restoration (Ikkala et al., 2022; Ball et al., 2023; Isoaho et al., 2023).

RS techniques have proven to be useful for upscaling field measurement data and for hydrological monitoring in the boreal peatlands (Harris and Bryant, 2009; Burdun et al., 2020b; Lees et al., 2021; Räsänen et al., 2022; Burdun et al., 2023). In general, optical, thermal, as well as passive and active microwave sensors have been used to track changes in the surface soil moisture; however, RS cannot directly observe belowground changes in wetness (Li et al., 2021; Peng et al., 2021). Nonetheless, in peatlands, it has been shown that the WT is often closely correlated with surface soil moisture due to the capillary connectivity (Lafleur et al., 2005; Strack and Price, 2009; Irfan et al., 2020) and also connected to the vegetation patterns (Breeuwer et al., 2009; Potvin et al., 2015), both of which can be tracked with RS (Meingast et al., 2014; Räsänen and Virtanen, 2019; Wigmore et al., 2019; Räsänen et al., 2020; Villoslada et al., 2023; Pang et al., 2023). In the same vein, recent studies from peatlands have indicated that optical imagery correlates well with the WT or soil moisture (Burdun et al., 2020b; Räsänen et al., 2022; Kolari et al., 2022; Burdun et al., 2023), and even better than microwave or thermal data (Burdun et al., 2020a; Räsänen et al., 2022). Nevertheless, synthetic aperture radar (SAR) observations have slightly improved the peatland water table modelling accuracy when utilised together with optical imagery (Räsänen et al., 2022). SAR imagery has also been used successfully to monitor WT and moisture dynamics in water-saturated environments (Bechtold et al., 2018; Millard and Richardson, 2018; Asmuß et al., 2019; Lees et al., 2021; Räsänen et al., 2022).

Of the optical variables, particularly, short-wave infrared (SWIR), near-infrared (NIR) and red reflection have been shown to be sensitive to changes in the peatland hydrology (Harris and Bryant, 2009; Kolari et al., 2022; Räsänen et al., 2022; Isoaho et al., 2023). Other spectral indices have been used with varying success (Meingast et al., 2014; Kolari et al., 2022; Isoaho et al., 2023). In some studies both vegetation and moisture indices have correlated with on-site moisture (Zhang et al., 2014; Kalacska et al., 2018; Šimanauskienė et al., 2019), while other studies have indicated that the index-moisture relationship is weak or non-existent (Kolari et al., 2022; Isoaho et al., 2023). Typically, the RS-based approaches for estimating WT have performed well in peatlands in which tree cover is sparse (Räsänen et al., 2022; Burdun et al., 2023), which is a typical trait for the central parts of large northern aapa mire complexes.

As restoration usually has large-scale hydrological impacts on peatlands, relevant changes in the WT can possibly be seen with a coarser spatial (>10 m) resolution. This enables the use of satellite imagery for temporal as well as spatial modelling (Kalacska et al., 2018; Burdun et al., 2020b; Räsänen et al., 2022; Jussila et al., 2023). Optical satellite imagery captured by Landsats 4–9 (L4–9) and Sentinel-2 (S2), and SAR satellite imagery captured by Sentinel-1 (S1), provide a sufficient spatial and temporal resolution for peatland monitoring (Räsänen et al., 2022). This provides an opportunity to assess the restoration impact remotely. However, spatiotemporal changes in the peatland hydrology, such as changes in the WT level, caused by the restoration have not been studied with multi-sensor satellite imagery before.

To address the knowledge gaps in the use of satellite imagery in the restoration monitoring, we construct a semi-automated machine learning approach for hydrological peatland restoration impact assessment using a combination of field measurement data and open access RS data. Our more specific objectives are as follows: (1) to examine how well the WT changes can be tracked with optical and radar satellite imagery, (2) to assess the spatial post-restoration WT change during high-water and low-water conditions, and (3) to statistically test the magnitude of the WT change in areas impacted by hydrological restoration and in control areas.

2. Methods

2.1. Study sites

We studied six restored open peatlands and five control sites in Finland in similar climatic conditions (Fig. 1, Table 1). Before restoration, all the studied sites were mostly unditched but suffering from adjacent drainage. In upper catchment areas of the sites, drainage is maintained at the peatlands and mineral soil lands that are used for forestry. While the upslope lands have discharged to the study sites in their former pristine state, ditching at the edge of the open peatlands has directed the upslope water flows past the study sites before their restoration. This has led to the intensification of tree growth near the edge ditches and to a significant decrease in the treeless peatland area. As a result, wet flarks (i.e. hollow depressions with almost permanent on-surface water) and *Carex* dominated vegetation has been replaced by *Sphagnum* dominated vegetation in large areas, which is a typical trend in the drainage-affected aapa mires in Finland (Granlund et al., 2022; Kolari et al., 2022; Kolari and Tahvanainen, 2023). Presumably, also the WT level has decreased due to the adjacent drainage.

While traditional restoration by blocking the ditches is appropriate for some parts of these sites, a more cost-efficient measure is to channel the waters from the upslope ditch network back to the restoration site by excavating water-directing ditches into the unditched parts of the peatlands. Four of our study sites have been restored by channelling water back to the peatland through new directing ditches and by blocking drainage (hereafter VESPA sites), and two of our study sites almost exclusively by ditch blocking (hereafter TRAD sites). However, due to the dense tree cover dominating most of the TRAD restoration sites, we have delineated our study areas to the lower (also unditched

Table 2
Used remote sensing bands and indices with the equations. Justifications for the different remote sensing variables are in Table S1.

Variable	Abbreviation	Equation	Reference
Blue reflectance	BLUE		
Green reflectance	GREEN		
Red reflectance	RED		
Near-infrared reflectance	NIR		
Shortwave infrared band 1 reflectance	SWIR1		
Shortwave infrared band 2 reflectance	SWIR2		
Shortwave infrared transformed reflectance	STR	$\frac{(1-SWIR1)^2}{2*SWIR1}$	Sadeghi et al., 2015
Normalised Difference Vegetation Index	NDVI	$\frac{NIR-RED}{NIR+RED}$	Tucker, 1979
Enhanced Vegetation Index	EVI	$2.5*\frac{NIR-RED}{NIR+6*RED-7.5*Blue+1}$	Liu and Huete, 1995
Soil Adjusted Vegetation Index	SAVI	$1.5*\frac{NIR-RED}{NIR+RED+0.5}$	Huete, 1988
Tasseled cap Greenness*	TCGreenness	$BLUE*(-0.2941)+GREEN*(-0.243)+RED*(-0.5424)+NIR*0.7276+SWIR1*0.0713+SWIR2*(-0.1608)$	Kauth and Thomas, 1976; Crist and Cicone, 1984
Normalised Difference Water Index	NDWI	$\frac{GREEN-NIR}{GREEN+NIR}$	McFeeters, 1996
Modified Normalised Difference Water Index	MNDWI	$\frac{GREEN-SWIR2}{GREEN+SWIR2}$	Xu, 2006
Normalised Difference Moisture Index	NDMI	$\frac{NIR-SWIR1}{NIR+SWIR1}$	Gao, 1996
Normalised Difference Moisture Index 2	NDMI2	$\frac{NIR-SWIR2}{NIR+SWIR2}$	Gao, 1996
Tasseled cap Wetness*	TCWetness	$BLUE*0.1511+GREEN*0.1973+RED*0.3283+NIR*0.3407+SWIR1*(-0.7117)+SWIR2*(-0.4559)$	Kauth and Thomas, 1976; Crist and Cicone, 1984
Tasseled cap Angle* and **	TCAngle	$arctan\left(\frac{TCGreenness}{TCBrightness}\right)$	Powell et al., 2010
Original VV backscatter	VV		
Sine corrected VV backscatter***	VV_sine	$VV-sin(0.023*(doy-140))$	Lees et al., 2021; Räsänen et al., 2022
Original VH backscatter	VH		
Sine corrected VH backscatter***	VH_sine	$VH-sin(0.023*(doy-140))$	Lees et al., 2021; Räsänen et al., 2022
Normalised polarisation of original backscatters	Pol	$\frac{VH-VV}{VH+VV}$	Becker and Choudhury, 1988
Normalised polarisation of sine corrected backscatters	Pol_sine	$\frac{VH\_sine-VV\_sine}{VH\_sine+VV\_sine}$	Becker and Choudhury, 1988; Räsänen et al., 2022

* Landsat OLI tasseled cap coefficients (Baig et al., 2014) are used because the data are harmonised to the OLI sensor.
** TCBrightness = BLUE * 0.3029 + GREEN * 0.2786 + RED * 0.4733 + NIR * 0.5599 + SWIR1 * 0.508 + SWIR2 * 0.1872.
*** doy is the day of the year of the observation.

and open) part of the peatlands, making the studied areas rather similar to that of VESPA sites. All restoring measures have been implemented during 2018–2021. We have selected the control sites so that they are geographically close to the restored ones and unrestored during the study period, and have a similar vegetation and land cover pattern as the restored ones before their restoration. We have five control sites since two restored sites (Haudanneva and Vihtaneva) are located near each other and have similar peatland ecosystem types; thus, the same control site (Latvaneva) is used for both of these sites.

The VESPA sites and their controls are drained but relatively wet aapa mires with clear microtopographic patterns of alternating wet flarks and drier strings on elevated positions. Part of the VESPA sites have previously been studied by Isoaho et al. (2023) but only in limited areas with drone imagery. The TRAD sites and their controls are smaller and located in the sloped, high ends of extensive aapa mire complexes; thus, they are drier than VESPA sites and their microtopographic structure is not as clear. The microtopography structure at the TRAD sites has partly disappeared because of the drainage impact. The TRAD sites and their controls have previously been studied by Ikkala et al. (2022), and we have followed their study area delineations.

2.2. Field reference data

We used two different field reference WT datasets from 2019 to 2023: manually measured data from VESPA sites and automatic logger data from TRAD sites. The total number of used field measurements was 268 (180 manual and 88 automatic logger measurements; Table 3). The WT was calculated in relation to local peatland surface, with a negative value indicating the levels below and a positive one above the surface. WT monitoring was carried out only at the restoration sites.

The manual WT measurements from perforated plastic pipes were conducted at VESPA sites during the growing seasons of 2021 (Haudanneva, Vahtisuo) and 2021–2023 (Vihtaneva, Kurkineva) 3–4 times each year (Table 3). Each measurement site had 6–12 permanent pipes in locations with large wetness variability (Fig. 1). During the spring 2023, we noticed that we lacked WT measurements from wet flarks; therefore, we conducted five extra measurements during the May 2023 field campaing at Kurkineva to complement the dataset. We also removed three field measurement points from the dataset because they were not representative of the surrounding landscape and might have disturbed the modelling that utilised relatively coarse spatial resolution satellite imagery (see Fig. 1). These points were located, for example, in

Table 3
Field measurement and used imagery dates (format YYYY-MM-DD) for the model construction, and number of utilised field measurements within the sites (n).

Haudanneva ($n = 15$)			Vahtisuo ($n = 18$)			Vihtaneva ($n = 69$)			Kurkineva ($n = 78$)			Iso Leväniemi ($n = 32$)	Loukkusuo ($n = 56$)
Field data	Optical	SAR	Field data	Optical	SAR	Field data	Optical	SAR	Field data	Optical	SAR	Monitoring period**	Monitoring period**
2021-05-24	2021-05-25	2021-05-25	2021-05-24	2021-05-30	2021-05-31	2021-05-24	2021-05-25	2021-05-25	2021-05-25	2021-05-30	2021-05-30	2019-07-20–2019-10-05	2019-05-30–2019-09-24
2021-07-17	2021-07-14	2021-07-13	2021-07-30	2021-07-28	2021-07-25	2021-07-16	2021-07-14	2021-07-13	2021-07-15	2021-07-09	2021-07-11	2020-05-20–2020-10-04	2020-06-03–2020-10-04
2021-10-06	2021-09-27	2021-09-27	2021-10-05	2021-09-27	2021-09-28	2021-10-06	2021-09-27	2021-09-27	2021-10-04	2021-09-27	2021-09-27		2021-06-01–2021-10-04
						2022-05-30	2022-06-06	2022-05-31	2022-05-30	2022-06-06	2022-06-07		2022-05-24–2022-08-09
						2022-07-15	2022-07-04	2022-07-06	2022-07-15	2022-07-21	2022-07-20		
						2022-08-19	2022-08-20	2022-08-23	2022-08-19	2022-08-20	2022-08-23		
						2022-10-07	–	–	2022-10-07	2022-09-24	2022-09-23		
						2023-05-29	2023-05-20 and 2023-06-14*	2023-06-02	2023-05-29	2023-05-20 and 2023-06-14*	2023-06-02		
						2023-07-12	2023-07-11	2023-07-13	2023-07-12	2023-07-11	2023-07-13		
						2023-10-03	2023-09-22	2023-09-23	2023-10-03	2023-09-22	2023-09-23		

* Time-weighted average between two images.
** All suitable Sentinel-2 images were used within the periods; suitability was manually checked for every image.

the middle of a narrow string or hummock surrounded by wet flarks.

The logger WT monitoring was conducted in TRAD sites during the growing seasons 2019–2022 (Fig. 1). Both sites had two loggers in place, but only one logger per site was in the open area suitable for RS methods; therefore, we only utilised one logger per site. Loggers collected data half-hourly, but we calculated daily averages for the analysis. We measured the WT level several times from the logger pipe within the monitoring periods to calibrate the data in relation to the peatland surface. The calibration was based on the average error between the automated and manual measurement.

2.3. Pre-processing of the satellite imagery

We utilised the GEE cloud computing platform (Gorelick et al., 2017) for processing and acquiring the S2 and L7–9 surface reflectance imagery, and S1 C-band SAR imagery to model changes in the WT. First, we filtered out optical imagery that had >30% cloud cover. Leftover clouds, cloud shadows and snow were masked out with Scene Land Cover and Quality Assessment pixel classification for S2 and L7–9, respectively. Second, to enable the use of data from different sensors in the analysis, we harmonised all imagery to the L8–9 OLI sensor with Roy et al. (2016) proposed coefficients and slopes for L7 and with Zhang et al. (2018) proposed coefficients and slopes for S2. Third, after cloud masking and harmonisation, we calculated a set of spectral indices previously used for peatland and other wetness studies (Table 2, Table S1). Finally, we calculated averages between duplicate dates within the dataset as multiple optical datasets had overlapping observations.

For S1, we included vertical transmit-vertical receive (VV) and vertical transmit-horizontal receive (VH) data only from ascending orbit and applied preprocessing steps suggested by Mullissa et al. (2021) to improve data quality. These included additional border noise correction, speckle reduction with multi-temporal (Quegan and Yu, 2001) Lee Sigma filter with kernel size and number of images set to 5, and radiometric terrain normalisation (Hoekman and Reiche, 2015; Vollrath et al., 2020) with 10 m spatial resolution Digital Elevation Model produced by National Land Survey of Finland. We also calculated sine corrected VV and VH backscatters (Lees et al., 2021) by using the equation that has been better matched with Finnish growing season (Räsänen et al., 2022; Table 2). Additionally, we calculated normalised polarisation (Pol) from the backscatters.

2.4. Modelling approach

To generate data for model calibration and validation, we searched for cloud-free S2 data that were temporally as close as possible to the field measurement data (Table 3). With the manual WT data, we used the closest dated image, but if a suitable image was not found, we calculated time-weighted averages between two images captured before and after the field data measurement date. With the logger data, we only utilised measurements from the dates where a cloud-free image was available. We checked S2 image quality, such as clouds, cloud shadows and other possible errors manually for every image that was used for the construction of the model. RS data were collected from the pixel where the measurement point was located. As the availability of optical data was more limited due to cloud cover, we prioritised days with optical observations and utilised S1 SAR observations that were as close as possible with the optical observations even if SAR observation was available during the field measurement day.

We used random forest regression (Breiman, 2001) for the modelling, with the field-measured WT being the response variable and satellite imagery metrics being the explanatory variables. Random forest was chosen due to its ability to deal with multiple multicollinear explanatory variables calculated from RS data (Belgiu and Drăguţ, 2016). We set the number of trees to 500 as typically the increase in performance diminishes and the model stabilises after a few hundred trees (Rodriguez-Galiano et al., 2012; Probst et al., 2019). We conducted

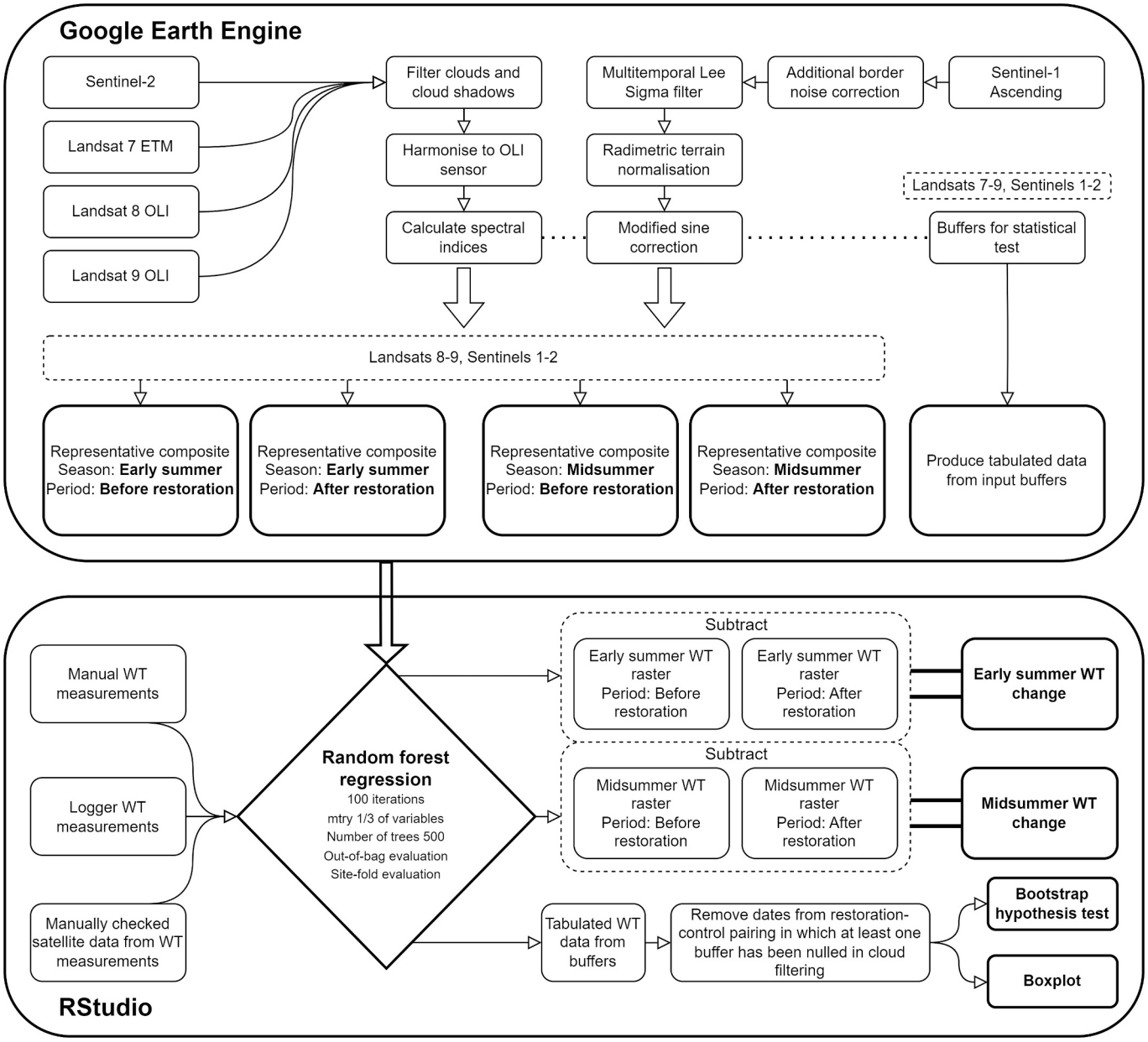

Fig. 2. Methodological flow chart. WT refers to water table. Spectral indices are explained in Table 2.

10-fold cross-validation tests for tuning the number of variables tested (mtry) at each node parameter. The tests indicated that the model performance was insensitive to mtry; thus, we set mtry to the 1/3 of all variables, i.e. the default value for the regression.

Finally, we assessed model performance with the out-of-bag (OOB) evaluation which has been reported to be a conservative estimate of model fit when compared to an independent test set (Clark et al., 2010). OOB utilises bootstrapped subsamples to train models and tests the fits with samples not used in training data. Additionally, we conducted site-specific validations by training the model with the data from all other sites than the testing site, to further assess the modelling performance. The performance metrics were coefficient of determination (R^2) and root-mean-square error (RMSE). We also extracted variable importance using % increase in mean square error statistic.

We repeated full-model and site-fold fits 100 times and calculated means of the fitted predictions, and produced the performance metrics from the means to flatten single-run randomness of random forest. We also calculated mean variable importance from 100 full models and normalised the values between 0 and 100. We conducted modelling separately for multi-sensor (optical and SAR), optical only, and SAR only determine effect of differenct sensors. Regressions were conducted with R (version 4.2.1) with the *randomForest* (Liaw and Wiener, 2022) package.

2.5. Restoration impact assessment

2.5.1. Spatiotemporal assessment with representative imagery

We assessed the spatial impact of restoration to the WT for two different time periods: the early summer in the beginning of the growing season (1 May – 15 June, hereafter ES) and the midsummer (1 July – 15 August, hereafter MS). The ES situation represents the time-point when the WT is typically at its highest right after the snowmelt (Sallinen et al., 2023). The MS situation represents the climax of the thermic summer with a high evaporation condition and when the WT is at its lowest due

Table 4
Number of buffer observations per site per year for filtered buffer data.

Study site/ Control site	2015	2016	2017	2018	2019	2020	2021	2022	2023
Haudanneva/ Latvaneva	72	120	120	528	312	288	480	336	384
Vahtisuo/ Salmensuo	72	24	240	696	336	528	384	456	360
Vihtaneva/ Latvaneva	108	216	180	792	432	396	684	504	612
Kurkineva/ Rimminneva	40	50	90	270	170	110	260	160	160
Iso Leväniemi/ Kirkaslampi	60	48	120	372	240	288	324	180	276
Loukkusuo/ Tammalampi	68	68	221	544	306	289	391	255	306

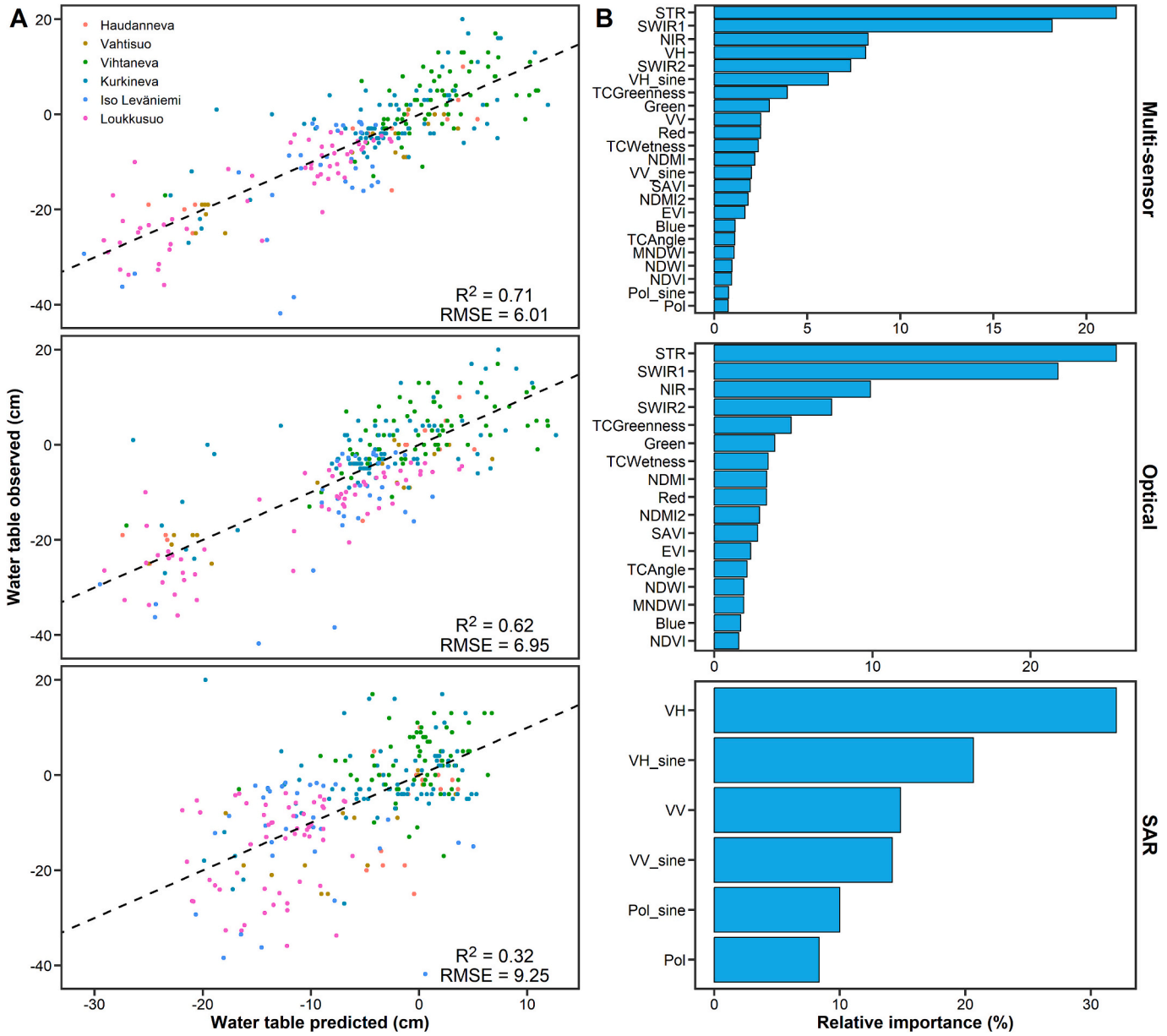

Fig. 3. Scatterplots between mean out-of-bag predicted over 100 fits and observed water tables with 1:1 line for different model types (A) and bar chart of the normalised relative variable importance (i.e. linearly scaled so that the sum of the importance of all variables equals 100) based on the increase in mean square error of the predictions for different model types over 100 fits (B).

Table 5
Site-specific mean multi-sensor model fits over 100 iterations. OOB refers to out-of-bag evaluation, R^2 to coefficient of determination, and RMSE to root-mean-square-error.

Site	Full model OOB R^2	Site-fold R^2	Full model OOB RMSE	Site-fold RMSE
Haudanneva	0.80	0.81	4.84	4.69
Vahtisuo	0.88	0.88	4.05	4.57
Vihtaneva	0.39	0.32	5.26	6.06
Kurkineva	0.50	0.31	6.13	8.59
Iso Leväniemi	0.44	0.27	9.16	10.45
Loukkusuo	0.71	0.74	5.22	6.57

to the low effective precipitation in the study region. Both time points are important for estimating the restoration impacts. The ES shows the maximum discharge directed to the area, while the MS shows the restoration impact when the water sources to peatland vegetation are the most limited.

To quantify spatial dynamics of the WT change, we constructed representative pixel-by-pixel imagery for both ES and MS situations describing average conditions before and after restoration by utilising multitemporal preprocessed L8–9 and S2 images for optical data (observations from 2013 onwards), and S1 for SAR data (observations from 2015 onwards). We did not include L7 for the composition because of the scan line corrector failure has led to striping of imagery, which could increase the uncertainty when producing representive spatial composites. For the optical imagery, we calculated pixel-by-pixel 40th percentile composites following the methodology of Pitkänen et al. (2024), who indicated that this construction strategy produces a better outcome than the more common median-based compilations as the latter might have more cloud fragments or haze and low-reflectance areas derived from cloud shadows that bypass the filters (Fig. 2). For the SAR imagery, we calculated medians, as the image quality is less affected by clouds and shadows. We derived representative images for control sites utilising same data collection years as for the corresponding restoration site and constructed all composites with nearest neighbour resampling in 10 m resolution. Finally, we predicted the WT from the representative imagery with the full regression model 100 times each, and calculated mean of the predicted WT rasters to again eliminate single-run randomness. To assess the change caused by restoration, we subtracted the before-restoration WT raster from the after-restoration WT raster and repeated the procedure separately for the ES and the MS situations.

2.5.2. Temporal assessment with a bootstrap test

To assess if the restoration increased WT with time-series data, and to produce uncertainty assessment within restoration-impacted areas, we conducted a bootstrap procedure test (Efron and Tibshirani, 1994). For this, we placed small buffers (radius 15 m, see Fig. 1) for restoration and control sites. In the VESPA sites, we placed the buffers' centres around 50 m from the end of every water-directing ditch towards the assumed direction of peatland water flow or around the same distance from filled drainage in a few hundred-metre intervals. In the TRAD sites, we placed the buffers also in treeless and filled drainage blocks. In the control sites, we sampled the buffer locations randomly around 50 m from the edges of study areas so that there were as many buffers as in the corresponding restoration site, except for Latvaneva which had two restoration counterparts; therefore, we calculated average between the number of buffers in two counterparts. By utilising multiple small buffers per site, we could more reliably assess the annual variations in the data, as well as flatten the variations caused by different pixel alignment of different optical datasets.

We tabulated the spectral bands, indices and SAR data for all preprocessed L7–9 and S1–2 images for the buffers during the snow-free periods (1 May – 31 October) for 2015–2023. We selected this period based on S1 availability and to see the multiyear variations. We also wanted to remove the effect of possible clouds that bypassed the filters as well as make the data between restoration site and its control as comparable as possible before the statistical testing. Thus, we only accepted dates where all buffers in the corresponding restoration and control site had spectral data. This filtering removed all the dates when masked cloud, cloud shadow, snow or L7 line stripe covered one or multiple buffers, leading to a more comparable dataset (Table 4). Finally, we utilised such SAR observations which were temporally as close as possible with the utilised optical observation. We used the multi-sensor regression model to predict WT from merged dataset 100 times and calculated the mean of predictions.

We used bootstrap procedure to test if the predicted WT before and after the restoration differed statistically significantly from each other and if the difference in the restoration buffers WT differed from that in the control buffers. Bootstrapping bypasses the distributional assumptions while keeping the test power high, making it suitable for our test setup. The approach creates a new sample from a given sample with replacement (here before and after restoration time periods, individually) and conducts a hypothesis test between two replaced samples. This is repeated 1000 times and, in each iteration, procedure calculates the test statistic and the difference between the sample means. As bootstrapping produces 1000 different results, we determined 95% confidence intervals for the test statistic and the mean difference in the samples and calculated the modified empirical *p*-value (Davison and Hinkley, 1997) from the results. We repeated the procedure for every buffer dataset individually.

3. Results

3.1. Model performance and variable importance

The constructed multi-sensor random forest regressions achieved an R^2 of 0.71 and an RMSE of 6.01 cm, while the separate models constructed from optical ($R^2 = 0.62$, RMSE = 6.95 cm) and SAR ($R^2 = 0.32$, RMSE = 9.25 cm) data achieved less accurate fits (Fig. 3A). The most important optical variables were STR and SWIR1 followed by NIR and SWIR2 (Fig. 3B). TCGreenness was the most important spectral index. From the SAR variables, VH and VH_sine were the most important ones, with VH outperforming the sine corrected version. The rest of the RS variables had small (<5%) contribution to the multi-sensor model.

Based on the site-specific validations, the models were able to predict values for the sites that were not used in the construction of the model with varying success ($R^2 = 0.27$–0.88, RMSE = 4.57–10.45 cm; Table 5), with the performance being close to but lower than the full model's site-specific out-of-bag estimates ($R^2 = 0.39$–0.88, RMSE = 4.05–9.16 cm; Table 5).

3.2. Spatial impact of the restoration

Both restoration methods (water-directing ditches and ditch blocking) had large local impacts on the WT of the restoration sites but they did not affect the WT universally, with differences within and between the sites (Fig. 4; Fig. 5). The control sites had changes in the predicted WT, but the spatial patterns were more random combared to the restored sites. There were also differences in the restoration impact between the ES and the MS. In general, the overall restoration impact to the entire peatland WT was moderately small, in most cases only an

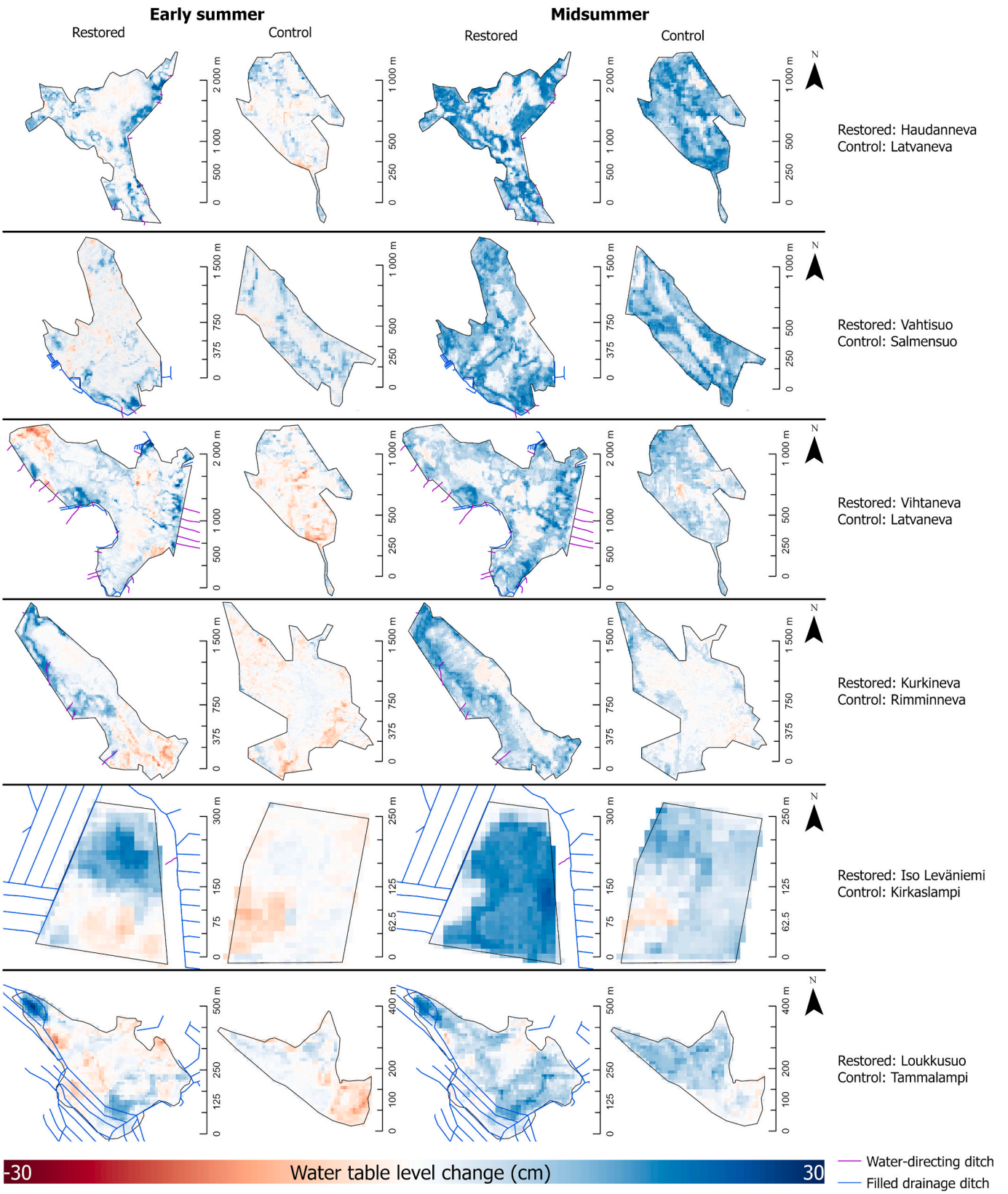

Fig. 4. Spatial water table level change of the study and control sites between before and after the restoration measures. Early summer refers to 1 May – 15 June and Midsummer to 1 July – 15 August. Conducted restoration measures are shown with lines.

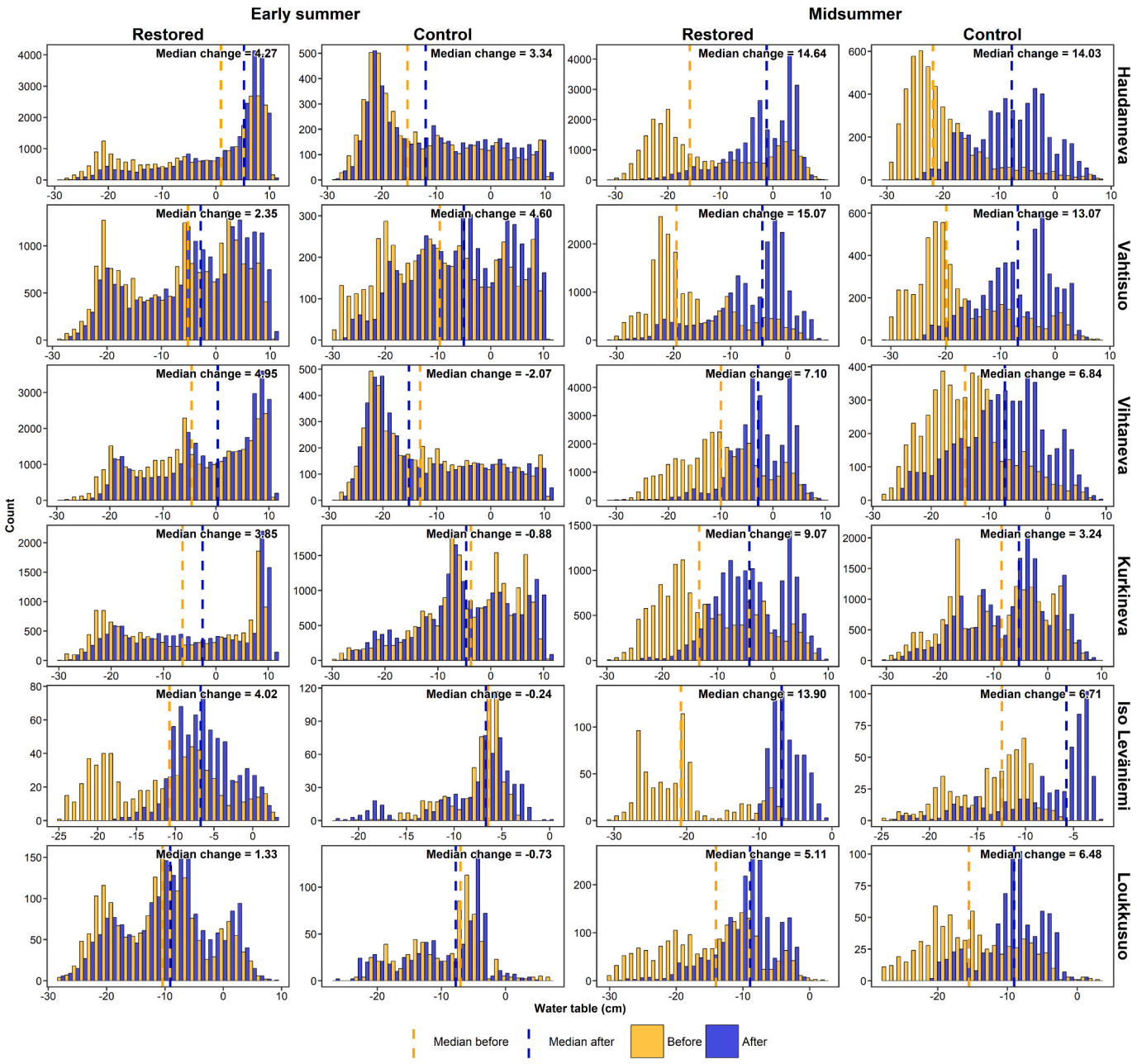

Fig. 5. Histograms of predicted water table rasters in restoration and corresponding control sites.

additional increase of a few cm compared to the control sites (Fig. 5).

By visually assessing the VESPA sites' WT change maps, the most impact on Haudanneva ES occurred in the north-east in which the WT increased up to 30 cm. The restoration also had an impact on the southern part of the peatland increasing the WT locally by 10–30 cm. Haudanneva's control site ES had no clear spatial patterns in the modelled WT change but had areas where the WT increased up to 21 cm. During the MS, the WT increased in the entire peatland area both in Haudanneva and the control without clear spatial patterns.

In Vahtisuo ES, there was a large impact caused by two water-directing ditches increasing the WT on average by 20–25 cm in a large area, while the impact of the most western ditch was lower. Ditch infilling increased the WT especially west of the water-directing ditches and some increase was visible on the eastern part of the peatland. Some increasing change on the WT was also visible in the northern part of the site although there are no restoration measures nearby. Vahtisuo's control site ES WT change varied between positive (20 cm increase) and negative (5 cm decrease) in the entire peatland area. During the MS, Vahtisuo results were very similar to Haudanneva.

In Vihtaneva, there were large-scale changes in the water supply as the restoration was implemented in multiple locations. WT increased across the peatland, with exceptions in some smaller areas. The western part of the peatland had large areas where restoration increased the WT up to 25 cm, both during the ES and the MS. Additionally, the south-eastern part near the ditch-infillings and water-directing ditches had a positive change in the WT for both periods. The five large water-directing ditches in the eastern part of the peatland functioned better during the ES than the MS. The control site's WT had a decreasing trend during the ES but small increasing trend without clear patterns during the MS.

At Kurkineva, restoration increased the WT in the north-western part of the peatland. The area around the end of the most northern water-directing ditch endpoint had the clearest positive, around 20 cm, change in the WT. The longest ditch in north-west had large impact,

Table 6
Bootstrapped hypothesis test results with the predicted water table buffer data from 2015 to 2023.

Restored site/Control site	Treatment buffer	Test statistic 95% confidence interval	Difference in mean	Difference 95% confidence interval	p-value
Haudanneva/Latvaneva	Restored	12.01–16.66	8.75	7.51–9.94	0.001
	Control	8.78–13.12	5.19	4.25–6.14	0.001
Vahtisuo/Salmensuo	Restored	10.61–15.17	5.72	4.86–6.58	0.001
	Control	6.23–10.36	3.81	2.91–4.74	0.001
Vihtaneva/Latvaneva	Restored	16.27–20.76	6.35	5.70–7.02	0.001
	Control	4.11–7.98	2.95	2.02–3.83	0.001
Kurkineva/Rimminneva	Restored	7.40–12.10	7.21	5.67–8.74	0.001
	Control	1.14–5.26	2.23	0.83–3.57	0.001
Iso Leväniemi/Kirkaslampi	Restored	9.45–13.70	6.04	5.03–7.03	0.001
	Control	0.73–4.69	1.19	0.34–2.14	0.005
Loukkusuo/Tammalampi	Restored	7.57–11.93	4.68	3.68–5.67	0.001
	Control	−1.83–2.02	0.07	−0.89–0.97	0.431

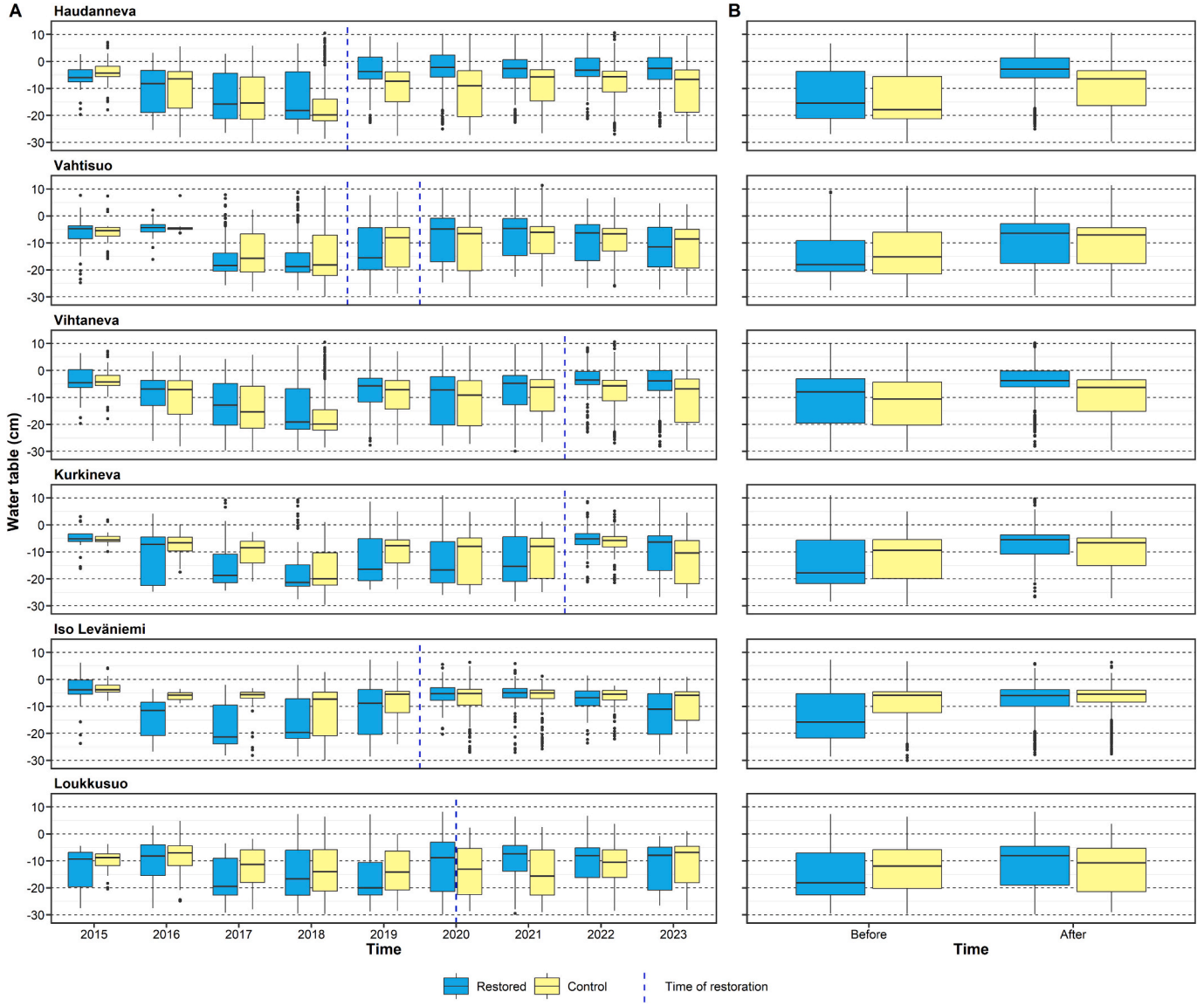

Fig. 6. Predicted water table within the constructed buffers at restoration and corresponding control sites in growing seasons of 2015–2023 (A) and summarised for before and after restoration (B). The more accurate time of restorations are explained in Table 1.

around 25 cm increase, both during the ES and the MS. Two ditches in the middle seemed to direct some water to the peatland during both of the time periods, increasing the WT from a few to 20 cm. The southern ditch might have led water to the peatland as there seemed to be a local increase in the WT during the ES, but it was hard to judge if this was caused by the restoration itself. Kurkineva's control site had decreasing WT changes during the ES and mild increases during the MS, but the spatial patterns were not as clear as in Kurkineva.

In the TRAD sites, the restoration had an increasing effect on the WT on a large spatial scale. Iso Leväniemi had a notable, 10–20 cm increase

in the WT in the northern part during the ES, but the entire site had a similar-scale increase during the MS. The control site had an opposite WT change during the ES but a somewhat similar but milder change during the MS.

Loukkusuo had two different key areas in the ES with a notable increase in the WT: ditch infilling areas in the western tip and southeastern part of the peatland, where the WT increased by 10–30 cm. During the MS, the increase in the WT occurred almost in the entire peatland area, but the same key areas had larger changes. The control site had similar but milder changes with a large WT increase during both time periods, but the control lacked clear spatial WT increase patterns.

3.3. Temporal impact on water table level

In every restoration treatment buffer, the predicted WT increased statistically significantly after the restoration measures based on the bootstrap test (p-value = 0.001; Table 6). In most of the cases, an increase in the control treatment also occurred. The increase was larger in the restoration treatments than in the controls in every study site pairing. The largest changes occurred in Haudanneva and Kurkineva, while the controls in the TRAD sites had the smallest changes.

By looking at the individual years (Fig. 6), the predicted WT increased in every restoration treatment during the restoration year or in the next growing season. Increase in the control treatment could be observed in the later part of monitoring period. In 2015 and 2016, the WT was universally high in the study sites. This was caused by a lack of drier midsummer images and a low overall number of images. Moreover, the year 2018 was a universally dry year in all sites.

4. Discussion

4.1. Modelling WT change with multi-sensor imagery

We have shown that spatial variation in WT can be predicted with optical and radar satellite imagery in open peatland areas with a relatively straightforward approach utilising a machine learning regression. Moreover, we have been able to show that our approach can be applied to detect peatland restoration impact to WT levels. This concurs with earlier studies by, e.g. Burdun et al. (2020a, 2020b, 2023) and Räsänen et al. (2022) who have successfully used optical satellite imagery to track temporal changes in open peatland WT. However, complementing the earlier studies, we have been able to illustrate that the spatial patterns in the WT change are not universal. Furthermore, our approach can be used in quantitative restoration impact assessment for detecting the hydrological impacted area of restoration. This is evidenced particularly by the relatively new restoration method of reconnecting aapa mires to their original watersheds through water-directing ditches, the effectiveness of which has not been widely analysed before (Isoaho et al., 2023). Therefore, we also show that in addition to traditional peatland restoration by ditch blocking, the water-directing ditch restoration is a valid method for the hydrological restoration of boreal aapa mires.

The constructed model had a relatively good predictive performance (R^2 = 0.39–0.88; RMSE = 4.04–9.16; overall R^2 = 0.71, RSME = 6.01). Additionally, the site-specific full model out-of-bag predictions varied from relatively poor to good (Table 5). The best fit was observed in sites in which the number of WT measurements was low and in which the field monitoring was conducted during one summer only, and in which the range of measurements was high (Haudanneva, Vahtisuo). In four other sites, the fit was poorer but the model was still able to produce a clear positive correlation with a rather small error between the observed and predicted WT. This was also the case with the site-specific validations as the performance metrics were generally similar but worse compared to the out-of-bag predictions. This is probably caused by site-specificity (e.g. Räsänen et al., 2022) and different WT measurement ranges between the sites, which challenges our approach to generate a universal modelling approach for WT prediction as random forest can not predict outside the training data WT range. Our results still indicate that the model can detect change in the WT even if the site is not included in the model construction, while the actual magnitude of the predicted WT change can be slightly biased. Being able to model outside the training sites supports the justification for our approach of utilising control sites that were not monitored in field as the control sites were needed to quantify the restoration impacts. This finding also opens possibilities to apply our model to large-scale spatial monitoring of similar boreal peatlands, but more validation sites are needed.

It has been suggested that the RS-based peatland WT prediction accuracy decreases when the site becomes drier. Burdun et al. (2023) have discussed that the relationship of the on-site WT and optical RS disappears after −40 cm, which is also in line with Räsänen et al. (2022) whose modelling approach functions better for wetter peatland sites. This is probably due to the lost capillary connections between the deeper WT and the peatland surface (Bechtold et al., 2018; Asmuß et al., 2019). The same phenomenon can be observed in our model (Fig. 3A) as the WT range for the prediction is around −30 to 10 cm, while the observed values ranged between −42 to 20 cm. In practice, this means that the WT levels of drained conditions prior the restoration might not be possible to estimate with RS if the site is well drained.

Our study produced further evidence that optical imagery seems to provide sufficient RS information for open peatland WT modelling, as optical variables were the most important, and the model constructed from optical variables performed nearly as well (R^2 = 0.62, RMSE = 6.95) as the multi-sensor model (R^2 = 0.71, RMSE = 6.01). Optical imagery does not directly reflect the WT, but it does observe changes in soil moisture, vegetation, and land cover, which are connected with WT dynamics (Lafleur et al., 2005; Breeuwer et al., 2009; Strack and Price, 2009; Potvin et al., 2015; Irfan et al., 2020). The dynamics can be visually interpreted from optical imagery as higher moisture causes reflectance values to decrease, making the areas darker (Chasmer et al., 2020). Still, multiple studies have suggested that SAR (Kim et al., 2017; Bechtold et al., 2018; Dabrowska-Zielinska et al., 2018; Millard and Richardson, 2018; Lees et al., 2021; Räsänen et al., 2022) or thermal imagery (Wigmore et al., 2019; Isoaho et al., 2023) could be used independently or combined with optical data to minimise prediction uncertainty. Our results partly support these findings as the combination of SAR and optical data produced the best estimates but the models using SAR data alone functioned much worse than the models using optical data. Nevertheless, a multi-sensor approach has limitations as the combination of multiple datasets decreases the temporal availability which is defined by the most sparse dataset and increases the processing work required for successful datamerging. Additionally it has been indicated that SAR can be utilised best when WT range is around −20 to −60 cm (Asmuß et al., 2019), making it less usable in highly saturated sites. In our case, most of the WT measurements were out of this range and the optical data functioned better than SAR; therefore optical imagery might be more practical for WT estimations in highly wet aapa mires and possibly in different wetland ecosystems. Also, by utilising only optical data, monitoring might be possible as far back as the 1980s with Landsat imagery.

As for the thermal satellite imagery, recent studies (Worrall et al., 2019, 2022) have demonstrated that land surface temperature from the MODIS TERRA satellite can be used to explain the post-restoration changes at the landscape scale. However, the highest spatial resolutions for northern latitudes are currently the 60 m resolution of L7, and 100 m of L8–9 thermal bands which might not be sufficient for the smaller spatial-scale restoration assessments. In addition to optical, SAR, and thermal data, also topographic data can be used in the restoration or degradation impact assessments (Carless et al., 2019; Ikkala et al., 2022), but the use of these data are limited by low temporal availability. Additionally, climatic variables have shown promise with the hydrological modelling of boreal peatlands (Gong et al., 2012; Sallinen et al., 2023). In the aapa mire context, ES WT is highly affected by snow melt

input, whereas MS WT is related to summer precipitation and evapotranspiration conditions (Sallinen et al., 2023). However, the currect spatial resolution of climatic grid (1 km; Aalto et al., 2016) is too coarse for detailed spatiotemporal modelling. Despite these restrictions, further tests with multi-source optical-SAR-thermal-climate approaches should be conducted in the future work.

Our methodological approach provides average WT change in a 10 m pixel size, but due to the relative coarse spatial resolution, the high spatial heterogeneity, a characteristic of northern peatlands (e.g. Räsänen and Virtanen, 2019), is lost. Higher spatial resolution RS imagery, e.g. from uncrewed aerial systems, could be utilised to provide more in-depth information about the restoration impacts (Ikkala et al., 2022; Isoaho et al., 2023). The higher resolution could also be utilised for example by capturing the RS spectral values within a small area around the measurement points and then harmonising this with coarse-resolution satellite imagery (Zhang and Zhao, 2019). The main challenge is labour intensity if a long-term time-series is aimed for even with a moderate temporal resolution.

Based on the variable importance information, single optical bands have contributed more than different spectral indices. This perhaps surprising result is in line with earlier studies (Kolari et al., 2022; Isoaho et al., 2023). Moreover, SWIR bands had the highest contribution, which is also a somewhat expected result as earlier work has had similar findings (Räsänen et al., 2022). The STR index, solely based on SWIR1 band (~1600 nm), has the highest variable importance of the separate variables. The STR index has recently been used for the assessment of aapa mires' "wetness" in the entire of northern Finland but without large-scale validation or comparison to other bands or indices (Jussila et al., 2023). Our results validate that STR can be used in peatland wetness monitoring. Therefore, our results indicate that single bands might provide enough information for the hydrological monitoring of open peatlands, and the use of indices utilising multiple bands or trapezoid models (Sadeghi et al., 2017; Burdun et al., 2023) is not necessarily needed. Additionally, the trapezoid models require model parameterisation, which makes them less straightforward to use than the simpler indices. Nevertheless, more research is needed to validate our findings, and to determine how well single bands function outside the aapa mires.

The lower importance of SAR compared to optical data is a somewhat expected result based on a previous study with a corresponding multi-sensor approach (Räsänen et al., 2022). Similar SAR explanatory capacity have been reported in some earlier studies (Bechtold et al., 2018; Asmuß et al., 2019; Räsänen et al., 2022), and our results reinforce these findings. We could have included more preprocessing steps to improve the quality of the SAR data, such as incidence angle corrections (Bechtold et al., 2018) but the method has only slightly improved the correlation between WT and SAR in boreal peatlands (Räsänen et al., 2022). Additionally, nonlocal pixel filtering (Manninen and Jääskelainen, 2022; Manninen et al., 2022) could be integrated into GEE and utilised in the future work.

Even though we have obtained promising results, our method is not entirely problem-free. As the capture of good-quality satellite images is hampered by cloud cover, we could not always merge the field data and satellite imagery dates as closely as would have been optimal. Additionally, our representative image strategy is heavily affected by a large number of observations from the extremely dry year of 2018 (Rinne et al., 2020; Jussila et al., 2023). This has probably led to post-restoration imagery (restored and control site) being modelled consistently wetter than pre-restoration in MS situations. Still, in most cases, the spatial patterns caused by restoration are still clearly apparent. However, in Haudanneva and Vahtisuo and their controls, this is not the case and the post-restoration patterns in the MS were unclear and messy. These possible modelling artifacts might be due to the time-periods utilised in the representative imagery; they were more affected by drought of 2018 compared to all other sites because the S2 imaging frequency was lower in 2017 compared to 2018 onwards, and L8 frequency was even lower, despite being available since 2013. In the future, the data availability might not be as apparent challenge, because S2 availability is nowadays high and proper pre-restoration imagery that captures multiyear variation can be constructed without outlier years.

4.2. Impact of the restoration

Based on our result maps, the increased water sources have the most evident effect near the water-directing ditches and infilled drainage. The non-uniform spatial patterns of post-restoration hydrological changes suggest that the restoration impact assessment should be conducted spatially either with abundant point-based measurements or wall-to-wall RS data. The non-uniformity also challenges the "best-pixel method" (Burdun et al., 2020b, 2023) in which the field-based WT data are linked to the satellite imagery pixel in the peatland area with the highest correlation with the WT measurement. As the "best-pixel" might not be located close to the WT measurement point, its temporal trends in the WT might be very different from that of the WT measurement, particularly after the restoration has been conducted.

In our study sites, the large flarks in the middle of the peatlands within the supposed water flow routes were modelled to be mostly unchanged after the restoration. There are multiple possible reasons for the observation. First, the model does not predict correctly the WT in the open water areas with a WT $>$ 10 cm (Fig. 3A). The difference in the relationship between the STR index and highly saturated soil compared to less saturated soil has been shown in laboratory conditions e.g. by Sadeghi et al. (2023). Additionally, random forest does, by nature, give conservative predictions to extreme values and cannot predict outside the training data value range (Coulston et al., 2016). Since we had a limited amount of high WT measurements, extreme values are not very accurately predicted. Another reason for the unchanged flarks could be that they already have a high WT level due to a large groundwater supply and therefore, they are not heavily impacted by drainage and possibly neither by restoration. Moreover, the restoration impact seems to be connected to the distance from the restoration measures, which is also partly visible in the study by Isoaho et al. (2023), and the most of the flarks are located far away from the measures.

The hydrological impact also differed between the sites. The clearest overall impact could be seen in the TRAD sites as the WT of the entire study sites increased (Fig. 4) and the bootstrap test showed a high difference between the before and after-restoration situations, while the controls had minor (Kirkaslampi) or statistically insignificant changes (Tammalampi; Table 6). This is backed by time-series data (Fig. 6) as the relationship between the treatments changes drastically after the restoration. In the VESPA sites, the changes were more local, while the overall changes of the sites were rather mild, only increases of few centimetres (Fig. 5). The local changes were more drastic and up to 30 cm WT increases were predicted at each VESPA site near the water-directing ditches (Fig. 4). The post-restoration increase in the WT has also been reported by multiple studies utilising continuous point-based monitoring with limited spatial coverage (Armstrong et al., 2010; Haapalehto et al., 2014; Menberu et al., 2016). In general, it seems that the average restoration impact on the entire peatland's WT is relatively minor, only a few cm increase (Fig. 4, Fig. 5).

The restoration impact assessment is often challenged by the within and between-year differences in the peatland hydrological conditions (e.g. Rinne et al., 2020; Lees et al., 2021; Jussila et al., 2023). Our results provide evidence for the spatial differences between the high-water ES and low-water MS situations (Fig. 4) and the overall WT differences between years (Fig. 6). As the hydrological conditions vary in time, the restoration impact assessment cannot be conducted with single time-point or even with single-year data; instead, the monitoring period should span multiple years. To further constrain uncertainties in the impact assessment judgement, also control sites need to be used. In our case, the partly limited monitoring period challenges our findings; part of the changes seen after restoration can potentially be attributed to the

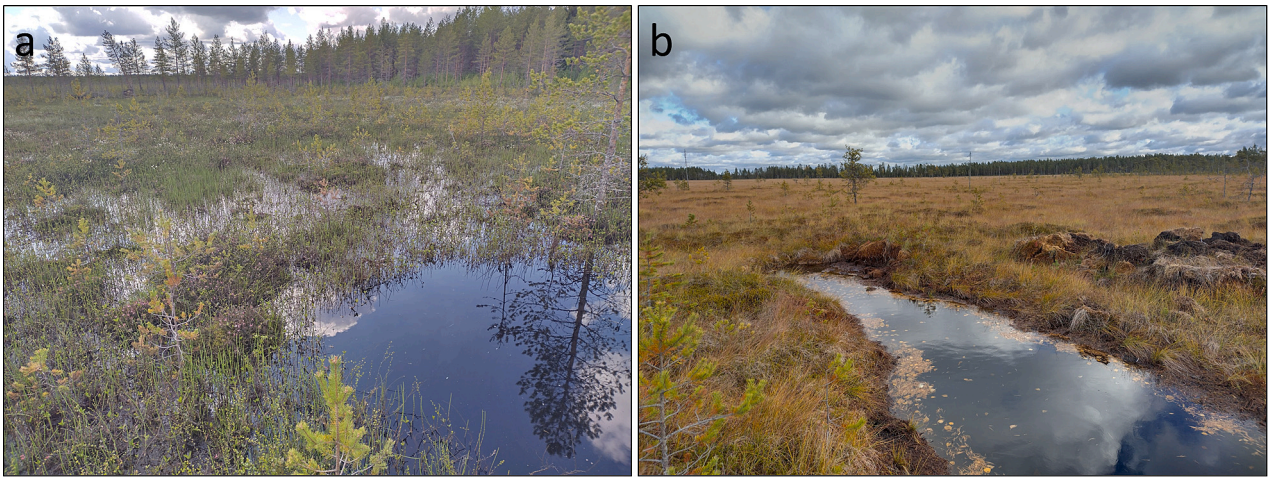

Fig. 7. Photographs at the endpoint of functional (a) and non-functional (b) water-directing ditches. Around a functional ditch, the WT is increased to a level near the peatland surface, while in the non-functional ditch, WT remains clearly underground and flow direction is unclear.

between-year variation as shown by the changes in the control sites. However, only a two-year monitoring after the restoration seemed to produce sufficient evidence about spatial WT changes in Vihtaneva and Kurkineva because hydrological changes can occur almost immediately after the restoration (Menberu et al., 2016).

A water-directing ditch should direct water to the peatland area causing a local rise in the WT (Fig. 4). Based on our models, this is not the case in all ditches. This also explains why the statistical test results (Table 4) did not show a higher difference between the before and after-restoration buffers in the VESPA sites; if we had chosen only the buffers in which the impact is large, the bootstrap test would have produced a larger change between the time periods. This is evident in Vihtaneva as there are water-directing ditches that brought only little water to the restoration site. This has also been noticed by the drone image analysis by Isoaho et al. (2023), according to whom there was no evident wetting effect at the end of every ditch. This has also been verified by visual interpretation in the field and with the photographs that show how some ditches were not directing water to the peatland (Fig. 7). However, functioning water-directing ditches have a high impact locally and also some impact on larger areas, suggesting that they area a valid restoration method.

We have shown that restoration measures have local impacts in peatland hydrology and that the measures can also in some cases cause changes in larger areas within the peatlands. Therefore, our method can be used to assess the impact area of the peatland restoration and for reporting the areal change in the hydrological status of the peatlands. Still, in addition of improving the hydrological function of a drained peatland, restoration is particularly targeted to improve the ecological status of peatlands. Therefore, the future studies could assess the ecological response, such as spread of *Carex* vegetation, to the changes in the hydrology and develop methods for assessing the spatiotemporal changes in peatland vegetation and habitats after the restoration.

5. Conclusion

We have developed and tested a new approach for spatiotemporal peatland restoration impact assessment on WT utilising optical and radar satellite imagery with machine learning. The constructed model has a relatively good explanatory capacity and it can be used to model spatial WT changes caused by restoration. Our results show that there are differences between and within the sites, but the highest hydrological impacts can be found near the actual restoration measures. Similar changes in WT have also been observed in the control sites but to a more limited magnitude and spatial extent. Additionally, our results support the assumed functionality of the water-directing ditches as a restoration measure. Overall, we suggest that the developed remote sensing approach can be used for peatland restoration monitoring and for the quantitative assessment of the hydrological impact area of the restoration sites.

CRediT authorship contribution statement

Aleksi Isoaho: Methodology, Investigation, Formal analysis, Conceptualization, Software, Validation, Visualization, Writing – original draft. **Lauri Ikkala:** Investigation, Writing – review & editing. **Lassi Päkkilä:** Investigation, Writing – review & editing. **Hannu Marttila:** Writing – review & editing, Supervision, Conceptualization. **Santtu Kareksela:** Writing – review & editing, Project administration, Funding acquisition, Conceptualization. **Aleksi Räsänen:** Writing – review & editing, Supervision, Project administration, Investigation, Funding acquisition, Conceptualization.

Declaration of competing interest

None.

Data availability

Data will be made available on request.

Acknowledgements

This study was funded by the Ministry of the Environment, Finland (VN/28337/2021-YM-2, VN/14352/2022, MetZo III project), Natural Resources Institute Finland (41007-00216200), European Union (LIFE16 NAT/FI/000 583) and Kone foundation (201710262). We thank Antti Räty for his advice regarding statistical analyses, Matti Salmela for checking the language, and Kaapro Keränen, Roosa Hautala and Otto Bigler for assisting in the field work. We also thank three anonymous reviewers for their valuable comments and suggestions which helped us to to improve the quality of the manuscript.

Appendix A. Supplementary data

Supplementary data to this article can be found online at https://doi.org/10.1016/j.rse.2024.114144.

References

Aalto, J., Pirinen, P., Jylhä, K., 2016. New gridded daily climatology of Finland: permutation-based uncertainty estimates and temporal trends in climate. J. Geophys. Res. Atmospheres 121, 3807–3823. https://doi.org/10.1002/2015JD024651.

Andersen, R., Farrell, C., Graf, M., Muller, F., Calvar, E., Frankard, P., Caporn, S., Anderson, P., 2017. An overview of the progress and challenges of peatland restoration in Western Europe: peatland restoration in Western Europe. Restor. Ecol. 25, 271–282. https://doi.org/10.1111/rec.12415.

Armstrong, A., Holden, J., Kay, P., Francis, B., Foulger, M., Gledhill, S., McDonald, A.T., Walker, A., 2010. The impact of peatland drain-blocking on dissolved organic carbon loss and discolouration of water; results from a national survey. J. Hydrol. 381, 112–120. https://doi.org/10.1016/j.jhydrol.2009.11.031.

Asmuß, T., Bechtold, M., Tiemeyer, B., 2019. On the potential of sentinel-1 for high resolution monitoring of water table dynamics in grasslands on organic soils. Remote Sens. (Basel) 11, 1659. https://doi.org/10.3390/rs11141659.

Autio, O., Jämsén, J., Rinkineva-Kantola, L., Joensuu, S., 2018. Veden palauttaminen kuivuneille suojelusoille kunnostusojituksen yhteydessä (No. 10/2018), Raportteja. ELY-keskus, Etelä-Pohjanmaan.

Baig, M.H.A., Zhang, L., Shuai, T., Tong, Q., 2014. Derivation of a tasselled cap transformation based on Landsat 8 at-satellite reflectance. Remote Sens. Lett. 5, 423–431. https://doi.org/10.1080/2150704X.2014.915434.

Ball, J., Gimona, A., Cowie, N., Hancock, M., Klein, D., Donaldson-Selby, G., Artz, R.R.E., 2023. Assessing the potential of using Sentinel-1 and 2 or high-resolution aerial imagery data with machine learning and data science techniques to model peatland restoration Progress – a northern Scotland case study. Int. J. Remote Sens. 44, 2885–2911. https://doi.org/10.1080/01431161.2023.2209916.

Bechtold, M., Schlaffer, S., Tiemeyer, B., De Lannoy, G., 2018. Inferring water table depth dynamics from ENVISAT-ASAR C-band backscatter over a range of peatlands from deeply-drained to natural conditions. Remote Sens. (Basel) 10, 536. https://doi.org/10.3390/rs10040536.

Becker, F., Choudhury, B.J., 1988. Relative sensitivity of normalized difference vegetation index (NDVI) and microwave polarization difference index (MPDI) for vegetation and desertification monitoring. Remote Sens. Environ. 24, 297–311. https://doi.org/10.1016/0034-4257(88)90031-4.

Belgiu, M., Drăguţ, L., 2016. Random forest in remote sensing: a review of applications and future directions. ISPRS J. Photogramm. Remote Sens. 114, 24–31. https://doi.org/10.1016/j.isprsjprs.2016.01.011.

Bonn, A., Allott, T., Evans, M., Joosten, H., Stoneman, R. (Eds.), 2016. Peatland Restoration and Ecosystem Services: Science, Policy and Practice, 1st ed. Cambridge University Press. https://doi.org/10.1017/CBO9781139177788.

Breeuwer, A., Robroek, B.J.M., Limpens, J., Heijmans, M.M.P.D., Schouten, M.G.C., Berendse, F., 2009. Decreased summer water table depth affects peatland vegetation. Basic Appl. Ecol. 10, 330–339. https://doi.org/10.1016/j.baae.2008.05.005.

Breiman, L., 2001. Random forests. Mach. Learn. 45, 5–32. https://doi.org/10.1023/A:1010933404324.

Burdun, I., Bechtold, M., Sagris, V., Komisarenko, V., De Lannoy, G., Mander, Ü., 2020a. A comparison of three trapezoid models using optical and thermal satellite imagery for water table depth monitoring in Estonian bogs. Remote Sens. (Basel) 12, 1980. https://doi.org/10.3390/rs12121980.

Burdun, I., Bechtold, M., Sagris, V., Lohila, A., Humphreys, E., Desai, A.R., Nilsson, M.B., De Lannoy, G., Mander, Ü., 2020b. Satellite determination of peatland water table temporal dynamics by localizing representative pixels of a SWIR-based moisture index. Remote Sens. (Basel) 12, 2936. https://doi.org/10.3390/rs12182936.

Burdun, I., Bechtold, M., Aurela, M., De Lannoy, G., Desai, A.R., Humphreys, E., Kareksela, S., Komisarenko, V., Liimatainen, M., Marttila, H., Minkkinen, K., Nilsson, M.B., Ojanen, P., Salko, S.-S., Tuittila, E.-S., Uuemaa, E., Rautiainen, M., 2023. Hidden becomes clear: optical remote sensing of vegetation reveals water table dynamics in northern peatlands. Remote Sens. Environ. 296, 113736 https://doi.org/10.1016/j.rse.2023.113736.

Carless, D., Luscombe, D.J., Gatis, N., Anderson, K., Brazier, R.E., 2019. Mapping landscape-scale peatland degradation using airborne lidar and multispectral data. Landsc. Ecol. 34, 1329–1345. https://doi.org/10.1007/s10980-019-00844-5.

Chapman, S., Buttler, A., Francez, A.-J., Laggoun-Défarge, F., Vasander, H., Schloter, M., Combe, J., Grosvernier, P., Harms, H., Epron, D., Gilbert, D., Mitchell, E., 2003. Exploitation of northern peatlands and biodiversity maintenance: a conflict between economy and ecology. Front. Ecol. Environ. 1, 525–532. https://doi.org/10.1890/1540-9295(2003)001[0525:EONPAB]2.0.CO;2.

Chasmer, L., Mahoney, C., Millard, K., Nelson, K., Peters, D., Merchant, M., Hopkinson, C., Brisco, B., Niemann, O., Montgomery, J., Devito, K., Cobbaert, D., 2020. Remote sensing of boreal wetlands 2: methods for evaluating boreal wetland ecosystem state and drivers of change. Remote Sens. (Basel) 12, 1321. https://doi.org/10.3390/rs12081321.

Clark, M.L., Aide, T.M., Grau, H.R., Riner, G., 2010. A scalable approach to mapping annual land cover at 250 m using MODIS time series data: a case study in the dry Chaco ecoregion of South America. Remote Sens. Environ. 114, 2816–2832. https://doi.org/10.1016/j.rse.2010.07.001.

Coulston, J.W., Blinn, C.E., Thomas, V.A., Wynne, R.H., 2016. Approximating prediction uncertainty for random Forest regression models. Photogramm. Eng. Remote. Sens. 82, 189–197. https://doi.org/10.14358/PERS.82.3.189.

Crist, E.P., Cicone, R.C., 1984. A physically-based transformation of thematic mapper data—the TM tasseled cap. IEEE Trans. Geosci. Remote Sens. GE-22, 256–263. https://doi.org/10.1109/TGRS.1984.350619.

Dabrowska-Zielinska, K., Musial, J., Malinska, A., Budzynska, M., Gurdak, R., Kiryla, W., Bartold, M., Grzybowski, P., 2018. Soil moisture in the Biebrza wetlands retrieved from Sentinel-1 imagery. Remote Sens. (Basel) 10, 1979. https://doi.org/10.3390/rs10121979.

Davison, A.C., Hinkley, D.V., 1997. Bootstrap Methods and their Application, 1st ed. Cambridge University Press. https://doi.org/10.1017/CBO9780511802843.

Efron, B., Tibshirani, R.J., 1994. An Introduction to the Bootstrap, 0 ed. Chapman and Hall/CRC. https://doi.org/10.1201/9780429246593.

European Commission, 2023. Nature Restoration Law [WWW Document]. Nat. Restor. Law. URL. https://environment.ec.europa.eu/topics/nature-and-biodiversity/nature-restoration-law_en (accessed 9.11.23).

Finnish Meteorological Institute, 2023. Daily observations in 1km*1km grid.

Gao, B., 1996. NDWI—A normalized difference water index for remote sensing of vegetation liquid water from space. Remote Sens. Environ. 58, 257–266. https://doi.org/10.1016/S0034-4257(96)00067-3.

Gong, J., Wang, K., Kellomäki, S., Zhang, C., Martikainen, P.J., Shurpali, N., 2012. Modeling water table changes in boreal peatlands of Finland under changing climate conditions. Ecol. Model. 244, 65–78. https://doi.org/10.1016/j.ecolmodel.2012.06.031.

Gorelick, N., Hancher, M., Dixon, M., Ilyushchenko, S., Thau, D., Moore, R., 2017. Google earth engine: planetary-scale geospatial analysis for everyone. Remote Sens. Environ. 202, 18–27. https://doi.org/10.1016/j.rse.2017.06.031.

Granlund, L., Vesakoski, V., Sallinen, A., Kolari, T.H.M., Wolff, F., Tahvanainen, T., 2022. Recent lateral expansion of Sphagnum bogs over central fen areas of boreal Aapa mire complexes. Ecosystems 25, 1455–1475. https://doi.org/10.1007/s10021-021-00726-5.

Haapalehto, T., Kotiaho, J.S., Matilainen, R., Tahvanainen, T., 2014. The effects of long-term drainage and subsequent restoration on water table level and pore water chemistry in boreal peatlands. J. Hydrol. 519, 1493–1505. https://doi.org/10.1016/j.jhydrol.2014.09.013.

Harris, A., Bryant, R.G., 2009. A multi-scale remote sensing approach for monitoring northern peatland hydrology: present possibilities and future challenges. J. Environ. Manage. 90, 2178–2188. https://doi.org/10.1016/j.jenvman.2007.06.025.

Hoekman, D.H., Reiche, J., 2015. Multi-model radiometric slope correction of SAR images of complex terrain using a two-stage semi-empirical approach. Remote Sens. Environ. 156, 1–10. https://doi.org/10.1016/j.rse.2014.08.037.

Holden, J., Evans, M.G., Burt, T.P., Horton, M., 2006. Impact of land drainage on peatland hydrology. J. Environ. Qual. 35, 1764–1778. https://doi.org/10.2134/jeq2005.0477.

Huete, A.R., 1988. A soil-adjusted vegetation index (SAVI). Remote Sens. Environ. 25, 295–309. https://doi.org/10.1016/0034-4257(88)90106-X.

Ikkala, L., Ronkanen, A.-K., Ilmonen, J., Similä, M., Rehell, S., Kumpula, T., Päkkilä, L., Klöve, B., Marttila, H., 2022. Unmanned aircraft system (UAS) structure-from-motion (SfM) for monitoring the changed flow paths and wetness in Minerotrophic peatland restoration. Remote Sens. (Basel) 14, 3169. https://doi.org/10.3390/rs14133169.

Irfan, M., Kurniawati, N., Ariani, M., Sulaiman, A., Iskandar, I., 2020. Study of groundwater level and its correlation to soil moisture on peatlands in South Sumatra. J. Phys. Conf. Ser. 1568, 012028 https://doi.org/10.1088/1742-6596/1568/1/012028.

Isoaho, A., Ikkala, L., Marttila, H., Hjort, J., Kumpula, T., Korpelainen, P., Räsänen, A., 2023. Spatial water table level modelling with multi-sensor unmanned aerial vehicle data in boreal aapa mires. Remote Sens. Appl. Soc. Environ. 32, 101059 https://doi.org/10.1016/j.rsase.2023.101059.

Itoh, M., Okimoto, Y., Hirano, T., Kusin, K., 2017. Factors affecting oxidative peat decomposition due to land use in tropical peat swamp forests in Indonesia. Sci. Total Environ. 609, 906–915. https://doi.org/10.1016/j.scitotenv.2017.07.132.

Jussila, T., Heikkinen, R.K., Anttila, S., Aapala, K., Kervinen, M., Aalto, J., Vihervaara, P., 2023. Quantifying wetness variability in aapa mires with Sentinel-2: towards improved monitoring of an EU priority habitat. Remote Sens. Ecol. Conserv. https://doi.org/10.1002/rse2.363 rse2.363.

Kalacska, M., Arroyo-Mora, J., Soffer, R., Roulet, N., Moore, T., Humphreys, E., Leblanc, G., Lucanus, O., Inamdar, D., 2018. Estimating peatland water table depth and net ecosystem exchange: a comparison between satellite and airborne imagery. Remote Sens. (Basel) 10, 687. https://doi.org/10.3390/rs10050687.

Kareksela, S., Haapalehto, T., Juutinen, R., Matilainen, R., Tahvanainen, T., Kotiaho, J.S., 2015. Fighting carbon loss of degraded peatlands by jump-starting ecosystem functioning with ecological restoration. Sci. Total Environ. 537, 268–276. https://doi.org/10.1016/j.scitotenv.2015.07.094.

Kareksela, S., Ojanen, P., Aapala, K., Haapalehto, T., Ilmonen, J., Koskinen, M., Laiho, R., Laine, A., Maanavilja, L., Marttila, H., Minkkinen, K., Nieminen, M., Ronkanen, A.-K., Sallantaus, T., Sarkkola, S., Tolvanen, A., Tuittila, E.-S., Vasander, H., 2021. Soiden ennallistamisen suoluonto-, vesistö-, ja ilmastovaikutukset. In: Vertaisarvioitu raportti. Suom. Luontopaneelin Julk. 2021/3b. https://doi.org/10.17011/jyx/SLJ/2021/3b.

Kauth, R.J., Thomas, G.S., 1976. The Tasselled Cap–a Graphic Description of the Spectral-Temporal Development of Agricultural Crops as Seen by Landsat, in: Proceedings of the Symposium on Machine Processing of Remotely Sensed Data. Purdue University, West Lafayette.

Kim, J.-W., Lu, Z., Gutenberg, L., Zhu, Z., 2017. Characterizing hydrologic changes of the great dismal swamp using SAR/InSAR. Remote Sens. Environ. 198, 187–202. https://doi.org/10.1016/j.rse.2017.06.009.

Kolari, T.H.M., Tahvanainen, T., 2023. Inference of future bog succession trajectory from spatial chronosequence of changing aapa mires. Ecol. Evol. 13, e9988 https://doi.org/10.1002/ece3.9988.

Kolari, T.H.M., Sallinen, A., Wolff, F., Kumpula, T., Tolonen, K., Tahvanainen, T., 2022. Ongoing Fen–Bog transition in a boreal aapa mire inferred from repeated field

sampling, aerial images, and landsat data. Ecosystems 25, 1166–1188. https://doi.org/10.1007/s10021-021-00708-7.
Lafleur, P.M., Moore, T.R., Roulet, N.T., Frolking, S., 2005. Ecosystem respiration in a cool temperate bog depends on peat temperature but not water table. Ecosystems 8, 619–629. https://doi.org/10.1007/s10021-003-0131-2.
Lees, K.J., Artz, R.R.E., Chandler, D., Aspinall, T., Boulton, C.A., Buxton, J., Cowie, N.R., Lenton, T.M., 2021. Using remote sensing to assess peatland resilience by estimating soil surface moisture and drought recovery. Sci. Total Environ. 761, 143312 https://doi.org/10.1016/j.scitotenv.2020.143312.
Leifeld, J., Menichetti, L., 2018. The underappreciated potential of peatlands in global climate change mitigation strategies. Nat. Commun. 9, 1071. https://doi.org/10.1038/s41467-018-03406-6.
Li, Z.-L., Leng, P., Zhou, C., Chen, K.-S., Zhou, F.-C., Shang, G.-F., 2021. Soil moisture retrieval from remote sensing measurements: current knowledge and directions for the future. Earth Sci. Rev. 218, 103673 https://doi.org/10.1016/j.earscirev.2021.103673.
Liaw, A., Wiener, M., 2022. randomForest: Breiman and Cutler's Random Forests for Classification and Regression [WWW Document]. URL. https://cran.r-project.org/web/packages/randomForest/index.html.
Liu, H.Q., Huete, A., 1995. A feedback based modification of the NDVI to minimize canopy background and atmospheric noise. IEEE Trans. Geosci. Remote Sens. 33, 457–465. https://doi.org/10.1109/TGRS.1995.8746027.
Manninen, T., Jääskelainen, E., 2022. Pixel based multitemporal Sentinel-1 SAR Despeckling PIMSAR. IEEE Geosci. Remote Sens. Lett. 19, 1–5. https://doi.org/10.1109/LGRS.2021.3065300.
Manninen, T., Jääskelainen, E., Lohila, A., Korkiakoski, M., Räsänen, A., Virtanen, T., Muhic, F., Marttila, H., Ala-Aho, P., Markovaara-Koivisto, M., Liwata-Kenttala, P., Sutinen, R., Hanninen, P., 2022. Very high spatial resolution soil moisture observation of heterogeneous subarctic catchment using nonlocal averaging and multitemporal SAR data. IEEE Trans. Geosci. Remote Sens. 60, 1–17. https://doi.org/10.1109/TGRS.2021.3109695.
Marttila, H., Karjalainen, S.-M., Kuoppala, M., Nieminen, M.L., Ronkanen, A.-K., Kløve, B., Hellsten, S., 2018. Elevated nutrient concentrations in headwaters affected by drained peatland. Sci. Total Environ. 643, 1304–1313. https://doi.org/10.1016/j.scitotenv.2018.06.278.
McFeeters, S.K., 1996. The use of the normalized difference water index (NDWI) in the delineation of open water features. Int. J. Remote Sens. 17, 1425–1432. https://doi.org/10.1080/01431169608948714.
Meingast, K.M., Falkowski, M.J., Kane, E.S., Potvin, L.R., Benscoter, B.W., Smith, A.M.S., Bourgeau-Chavez, L.L., Miller, M.E., 2014. Spectral detection of near-surface moisture content and water-table position in northern peatland ecosystems. Remote Sens. Environ. 152, 536–546. https://doi.org/10.1016/j.rse.2014.07.014.
Menberu, M.W., Tahvanainen, T., Marttila, H., Irannezhad, M., Ronkanen, A.-K., Penttinen, J., Kløve, B., 2016. Water-table-dependent hydrological changes following peatland forestry drainage and restoration: analysis of restoration success. Water Resour. Res. 52, 3742–3760. https://doi.org/10.1002/2015WR018578.
Millard, K., Richardson, M., 2018. Quantifying the relative contributions of vegetation and soil moisture conditions to polarimetric C-band SAR response in a temperate peatland. Remote Sens. Environ. 206, 123–138. https://doi.org/10.1016/j.rse.2017.12.011.
Mullissa, A., Vollrath, A., Odongo-Braun, C., Slagter, B., Balling, J., Gou, Y., Gorelick, N., Reiche, J., 2021. Sentinel-1 SAR backscatter analysis ready data preparation in Google earth engine. Remote Sens. (Basel) 13, 1954. https://doi.org/10.3390/rs13101954.
Nieminen, M., Sallantaus, T., Ukonmaanaho, L., Nieminen, T.M., Sarkkola, S., 2017. Nitrogen and phosphorus concentrations in discharge from drained peatland forests are increasing. Sci. Total Environ. 609, 974–981. https://doi.org/10.1016/j.scitotenv.2017.07.210.
Pang, Y., Räsänen, A., Juselius-Rajamäki, T., Aurela, M., Juutinen, S., Väliranta, M., Virtanen, T., 2023. Upscaling field-measured seasonal ground vegetation patterns with Sentinel-2 images in boreal ecosystems. Int. J. Remote Sens. 44, 4239–4261. https://doi.org/10.1080/01431161.2023.2234093.
Peng, J., Albergel, C., Balenzano, A., Brocca, L., Cartus, O., Cosh, M.H., Crow, W.T., Dabrowska-Zielinska, K., Dadson, S., Davidson, M.W.J., De Rosnay, P., Dorigo, W., Gruber, A., Hagemann, S., Hirschi, M., Kerr, Y.H., Lovergine, F., Mahecha, M.D., Marzahn, P., Mattia, F., Musial, J.P., Preuschmann, S., Reichle, R.H., Satalino, G., Silgram, M., Van Bodegom, P.M., Verhoest, N.E.C., Wagner, W., Walker, J.P., Wegmüller, U., Loew, A., 2021. A roadmap for high-resolution satellite soil moisture applications – confronting product characteristics with user requirements. Remote Sens. Environ. 252, 112162 https://doi.org/10.1016/j.rse.2020.112162.
Pitkänen, T.P., Balazs, A., Tuominen, S., 2024. Automatized Sentinel-2 mosaicking for large area forest mapping. Int. J. Appl. Earth Obs. Geoinformation 127, 103659. https://doi.org/10.1016/j.jag.2024.103659.
Potvin, L.R., Kane, E.S., Chimner, R.A., Kolka, R.K., Lilleskov, E.A., 2015. Effects of water table position and plant functional group on plant community, aboveground production, and peat properties in a peatland mesocosm experiment (PEATcosm). Plant and Soil 387, 277–294. https://doi.org/10.1007/s11104-014-2301-8.
Powell, S.L., Cohen, W.B., Healey, S.P., Kennedy, R.E., Moisen, G.G., Pierce, K.B., Ohmann, J.L., 2010. Quantification of live aboveground forest biomass dynamics with Landsat time-series and field inventory data: a comparison of empirical modeling approaches. Remote Sens. Environ. 114, 1053–1068. https://doi.org/10.1016/j.rse.2009.12.018.
Prevost, M., Belleau, P., Plamondon, A.P., 1997. Substrate conditions in a treed peatland: responses to drainage. Écoscience 4, 543–554. https://doi.org/10.1080/11956860.1997.11682434.
Probst, P., Wright, M.N., Boulesteix, A., 2019. Hyperparameters and tuning strategies for random forest. WIREs Data Min. Knowl. Discov. 9, e1301 https://doi.org/10.1002/widm.1301.
Quegan, S., Yu, J.J., 2001. Filtering of multichannel SAR images. IEEE Trans. Geosci. Remote Sens. 39, 2373–2379. https://doi.org/10.1109/36.964973.
Räsänen, A., Virtanen, T., 2019. Data and resolution requirements in mapping vegetation in spatially heterogeneous landscapes. Remote Sens. Environ. 230, 111207 https://doi.org/10.1016/j.rse.2019.05.026.
Räsänen, A., Juutinen, S., Kalacska, M., Aurela, M., Heikkinen, P., Mäenpää, K., Rimali, A., Virtanen, T., 2020. Peatland leaf-area index and biomass estimation with ultra-high resolution remote sensing. GIScience Remote Sens. 57, 943–964. https://doi.org/10.1080/15481603.2020.1829377.
Räsänen, A., Tolvanen, A., Kareksela, S., 2022. Monitoring peatland water table depth with optical and radar satellite imagery. Int. J. Appl. Earth Obs. Geoinformation 112, 102866. https://doi.org/10.1016/j.jag.2022.102866.
Rinne, J., Tuovinen, J.-P., Klemedtsson, L., Aurela, M., Holst, J., Lohila, A., Weslien, P., Vestin, P., Łakomiec, P., Peichl, M., Tuittila, E.-S., Heiskanen, L., Laurila, T., Li, X., Alekseychik, P., Mammarella, I., Ström, L., Crill, P., Nilsson, M.B., 2020. Effect of the 2018 European drought on methane and carbon dioxide exchange of northern mire ecosystems. Philos. Trans. R. Soc. B Biol. Sci. 375, 20190517. https://doi.org/10.1098/rstb.2019.0517.
Rodriguez-Galiano, V.F., Ghimire, B., Rogan, J., Chica-Olmo, M., Rigol-Sanchez, J.P., 2012. An assessment of the effectiveness of a random forest classifier for land-cover classification. ISPRS J. Photogramm. Remote Sens. 67, 93–104. https://doi.org/10.1016/j.isprsjprs.2011.11.002.
Roy, D.P., Kovalskyy, V., Zhang, H.K., Vermote, E.F., Yan, L., Kumar, S.S., Egorov, A., 2016. Characterization of Landsat-7 to Landsat-8 reflective wavelength and normalized difference vegetation index continuity. Remote Sens. Environ. 185, 57–70. https://doi.org/10.1016/j.rse.2015.12.024.
Sadeghi, M., Jones, S.B., Philpot, W.D., 2015. A linear physically-based model for remote sensing of soil moisture using short wave infrared bands. Remote Sens. Environ. 164, 66–76. https://doi.org/10.1016/j.rse.2015.04.007.
Sadeghi, M., Babaeian, E., Tuller, M., Jones, S.B., 2017. The optical trapezoid model: a novel approach to remote sensing of soil moisture applied to Sentinel-2 and Landsat-8 observations. Remote Sens. Environ. 198, 52–68. https://doi.org/10.1016/j.rse.2017.05.041.
Sadeghi, M., Mohamadzadeh, N., Liang, L., Bandara, U., Caldas, M.M., Hatch, T., 2023. A new variant of the optical trapezoid model (OPTRAM) for remote sensing of soil moisture and water bodies. Sci. Remote Sens. 8, 100105 https://doi.org/10.1016/j.srs.2023.100105.
Sallinen, A., Tuominen, S., Kumpula, T., Tahvanainen, T., 2019. Undrained peatland areas disturbed by surrounding drainage: a large scale GIS analysis in Finland with a special focus on aapa mires. Mires Peat 1–22. https://doi.org/10.19189/MaP.2018.AJB.391.
Sallinen, A., Akanegbu, J., Marttila, H., Tahvanainen, T., 2023. Recent and future hydrological trends of aapa mires across the boreal climate gradient. J. Hydrol. 617, 129022 https://doi.org/10.1016/j.jhydrol.2022.129022.
Šimanauskienė, R., Linkevičienė, R., Bartold, M., Dąbrowska-Zielińska, K., Slavinskienė, G., Veteikis, D., Taminskas, J., 2019. Peatland degradation: the relationship between raised bog hydrology and normalized difference vegetation index. Ecohydrology 12. https://doi.org/10.1002/eco.2159.
Strack, M., Price, J.S., 2009. Moisture controls on carbon dioxide dynamics of peat-*Sphagnum* monoliths. Ecohydrology 2, 34–41. https://doi.org/10.1002/eco.36.
Tahvanainen, T., 2011. Abrupt ombrotrophication of a boreal aapa mire triggered by hydrological disturbance in the catchment: Ombrotrophication of aapa mires. J. Ecol. no-no. https://doi.org/10.1111/j.1365-2745.2010.01778.x.
Tucker, C.J., 1979. Red and photographic infrared linear combinations for monitoring vegetation. Remote Sens. Environ. 8, 127–150. https://doi.org/10.1016/0034-4257(79)90013-0.
Villoslada, M., Ylänne, H., Juutinen, S., Kolari, T.H.M., Korpelainen, P., Tahvanainen, T., Wolff, F., Kumpula, T., 2023. Reindeer control over shrubification in subarctic wetlands: spatial analysis based on unoccupied aerial vehicle imagery. Remote Sens. Ecol. Conserv. https://doi.org/10.1002/rse2.337 rse2.337.
Vollrath, A., Mullissa, A., Reiche, J., 2020. Angular-based radiometric slope correction for Sentinel-1 on Google earth engine. Remote Sens. (Basel) 12, 1867. https://doi.org/10.3390/rs12111867.
Whittington, P.N., Price, J.S., 2006. The effects of water table draw-down (as a surrogate for climate change) on the hydrology of a fen peatland. Canada. Hydrol. Process. 20, 3589–3600. https://doi.org/10.1002/hyp.6376.
Wigmore, O., Mark, B., McKenzie, J., Baraer, M., Lautz, L., 2019. Sub-metre mapping of surface soil moisture in proglacial valleys of the tropical Andes using a multispectral unmanned aerial vehicle. Remote Sens. Environ. 222, 104–118. https://doi.org/10.1016/j.rse.2018.12.024.
Wilkinson, S.L., Andersen, R., Moore, P.A., Davidson, S.J., Granath, G., Waddington, J. M., 2023. Wildfire and degradation accelerate northern peatland carbon release. Nat. Clim. Change. https://doi.org/10.1038/s41558-023-01657-w.
Worrall, F., Boothroyd, I.M., Gardner, R.L., Howden, N.J.K., Burt, T.P., Smith, R., Mitchell, L., Kohler, T., Gregg, R., 2019. The impact of peatland restoration on local climate: restoration of a cool Humid Island. J. Geophys. Res. Biogeo. 124, 1696–1713. https://doi.org/10.1029/2019JG005156.
Worrall, F., Howden, N.J.K., Burt, T.P., Rico-Ramirez, M.A., Kohler, T., 2022. Local climate impacts from ongoing restoration of a peatland. Hydrol. Process. 36, e14496 https://doi.org/10.1002/hyp.14496.
Xu, H., 2006. Modification of normalised difference water index (NDWI) to enhance open water features in remotely sensed imagery. Int. J. Remote Sens. 27, 3025–3033. https://doi.org/10.1080/01431160600589179.

Xu, J., Morris, P.J., Liu, J., Holden, J., 2018. PEATMAP: refining estimates of global peatland distribution based on a meta-analysis. CATENA 160, 134–140. https://doi.org/10.1016/j.catena.2017.09.010.

Zhang, S., Zhao, G., 2019. A harmonious satellite-unmanned aerial vehicle-ground measurement inversion method for monitoring salinity in coastal saline soil. Remote Sens. (Basel) 11, 1700. https://doi.org/10.3390/rs11141700.

Zhang, W., Lu, Q., Song, K., Qin, G., Wang, Y., Wang, X., Li, Hongxia, Li, J., Liu, G., Li, Hua, 2014. Remotely sensing the ecological influences of ditches in Zoige peatland, eastern Tibetan plateau. Int. J. Remote Sens. 35, 5186–5197. https://doi.org/10.1080/01431161.2014.939779.

Zhang, H.K., Roy, D.P., Yan, L., Li, Z., Huang, H., Vermote, E., Skakun, S., Roger, J.-C., 2018. Characterization of sentinel-2A and Landsat-8 top of atmosphere, surface, and nadir BRDF adjusted reflectance and NDVI differences. Remote Sens. Environ. 215, 482–494. https://doi.org/10.1016/j.rse.2018.04.031.